CHEMICAL MONITORING OF THE IN-SITU LEACHING OF A SOUTH TEXAS URANIUM OREBODY

R. W. Potter, II, M. A. Clynne, J. M. Thompson
V. L. Thurmond, R. C. Erd, N. L. Nehring, K. A. Smith,
P. J. Lamothe, and J. L. Seeley

U.S. Geological Survey, Menlo Park, California 94025

D. R. Tweeton, G. R. Anderson, and W. H. Engelmann

U.S. Bureau of Mines, Twin Cities, Minn.

Open-File Report 79-1144

This report is preliminary and has not been edited or reviewed for conformity with Geological Survey standards and nomenclature.

This report is a summary of work done by the U.S. Geological Survey under a contract from the U.S. Bureau of Mines

CONTENTS

CONTENTS (continued)

FIGURES (continued)

INTRODUCTION

In-situ leaching of orebodies is an extraction technology that has the potential of being an economical method of ore extraction as well as being the method that has the least adverse impact on the environment. Currently, large-scale extraction of uranium is being done economically by in-situ technology. To date, all large-scale in-situ leaching of uranium orebodies has been confined to southwest Texas; however, the imminent spread of this type mining to other states is indicated from pilot tests being conducted in other areas. Despite the successful application of in-situ leaching technology to the extraction of uranium, many features of the leaching process are not fully understood.

In order to elucidate the process of the in-situ leaching of uranium as well as to provide tests of various components used in in-situ leaching, the U.S. Bureau of Mines (USBM) initiated a cooperative monitoring test of a commercial in-situ leach operation in south Texas. The U.S. Geological Survey (USGS) was asked by the USBM to participate in the project in order to provide expertise in the geochemistry and mineralogy of the process. It was hoped that by augmenting the project with these types of data, information would be obtained that would aid in increasing recoveries and lessening any adverse impacts on the environment. This report is a summary of the data collected.

The geochemical and mineralogic data collection was broken down into two separate phases. The first phase, baseline data collection, consisted of establishing the initial conditions of the host rock and formation waters prior to the introduction of any lixiviant. This baseline characterization included the comprehensive mineralogy of the core samples obtained by the USBM from the leaching pattern and water analyses of the formation waters in the leaching pattern as well as from peripheral monitoring wells. The second phase involved the collection of comprehensive chemical data on the composition of the formation waters as a function of time during the leaching of the orebody. In addition to the geochemical and mineralogic data collected during these basic phases, performance data on field analytical methods, sampling and preservation methods, and on a downhole, gas-tight sampler were obtained. Such performance data are applicable for setting standards for the collection and analysis of samples, in order that standardized and meaningful chemical data may be obtained for purposes of requiring comparison, such as are involved in environmental questions.

BASELINE CHARACTERIZATION

Mineralogy of the Host Formation

The USBM provided core samples of the host formation. These samples consisted of four sections of sandstone (USBM-2, USBM-4, USBM-7, and USBM-8) and one section of the upper shale unit (USBM-2a). General data for the four samples of uraniferous sands studied are reported in table 1. All weight percentages shown are proportions of the entire sample used (rather than proportions of a particular mesh size or gravity fraction) so that each entry may be directly compared and its importance to the overall sample assessed. Colors and sample weights were noted for the samples as received and when dry. Approximately 10 g of each sample was removed for reference and later checks. A whole-rock X-ray diffraction pattern was then made using about 0.7 g of each sample. Clay minerals were separated using distilled water and oriented slides were prepared for X-ray study. The decanted water was evaporated in order to identify the water-soluble minerals present. Examination of the carbonates in the core material both optically and by X-ray revealed them to be essentially $CaCO_3$, hence the calcite content was determined by leaching it from the samples with 1:10 HCl. The remaining sand fraction was size-sorted by sieving. The -40 +80 mesh fraction of each of the samples was further separated using heavy liquids. X-ray and optical studies were then carried out for each fraction and for some minerals handpicked for special study.

Table 1. Data for samples of uraniferous sands from Texas

Sample number	USBM-2		USBM-4		USBM-7		USBM-8	
Color (damp)	pale olive gray 5Y 6/2		olive gray 5Y 4/1		light olive gray 5Y 5/2		medium olive gray 5Y 5/1	
Color (dry)	yellowish-gray 5Y 7/2		pale olive gray 5Y 6/2		pale olive gray 5Y 6/2		pale olive gray 5Y 6/2	
Sample Weight								
(as rec'd; g)	270.0		196.0		187.1		164.9	
(dry; g)	254.6		186.1		178.1		152.8	
H_2O^- (Weight %)	5.7		5.0		4.8		7.3	
	Wt. (g)	Wt. %	Wt. (g)	Wt. %	Wt. (g)	Wt. %	Wt. (g)	Wt. %
Study sample	234.4		175.2		166.7		142.3	
Clay minerals	23.4	9.6	12.3	7.0	11.3	6.8	9.1	6.4
Water soluble	0.2	0.1	0.2	0.1	0.2	0.1	0.2	0.1
Calcite	33.8	13.9	15.7	9.0	18.7	11.2	13.0	9.1
Sand (all other)	*186.0*	*76.4*	*147.0*	*83.9*	*136.5*	*81.9*	*120.0*	*84.3*
Total	243.4	100.0	175.2	100.0	166.7	100.0	142.3	99.9
Sand (Mesh size)								
+20	0.0	0.0	0.1	<0.1	0.0	0.0	0.0	0.0
-20 +40	5.6	2.3	8.5	4.8	1.2	0.7	2.2	1.5
-40 +80	*142.4*	*58.5*	*120.3*	*68.7*	*93.4*	*56.0*	*105.3*	*74.0*
-80 +120	25.1	10.3	11.0	6.3	21.7	13.0	5.9	4.1
-120	12.9	5.3	7.1	4.1	20.1	12.1	6.6	4.6
Total	186.0	76.4	147.0	83.9	136.4	81.8	120.0	84.2
Sand (-40 +80)								
Specific gravity								
<2.28	1.9	0.8	0.1	<0.1	0.1	<0.1	0.0_3	<0.1
2.28-2.57	46.0	18.9	12.1	6.9	13.7	8.2	4.2	3.0
2.57-2.62	63.2	26.0	11.1	6.3	15.8	9.5	16.3	11.4
2.62-2.67	27.2	11.2	93.2	53.2	58.5	35.1	82.4	57.9
2.67-2.85	2.7	1.1	2.8	1.6	4.4	2.6	1.6	1.1
2.85-3.31	1.4	0.5	0.7	0.4	0.4	0.2	0.4	0.3
>3.31	—	—	0.3	0.2	0.4	0.2	0.4	0.3
Total	142.4	58.5	120.3	68.6	93.3	55.8	105.3	74.0

Table 1a. Mineralogy of uraniferous sands.
Values in weight percent.

	USBM 2	USBM 4	USBM 7	USBM 8
Quartz	53	55	49	59
K-feldspar	12	13	15	12
Plagioclase	11	12	16	12
Calcite	13.9	9.0	11.2	9.1
Clays	7.4	7.0	6.8	6.4
Pyrite	1.2	1.5	.4	.6
Clinoptilolite	2	2	1.5	1.0

All of the four sand samples studied are similar to each other. Clay minerals are chiefly Ca-montmorillonite with subordinate, randomly-interstratified chlorite and illite. Calcite, quartz, pyrite, feldspars, and clinoptilolite are also present in minor amounts in the clay-size fraction. The water-soluble salts precipitated from the distilled-water leach were invariably found to be gypsum with minor calcite and halite. No gypsum was found in any of the sand samples, however. All of the water-soluble fractions gave positive tests for boron. Based on these observations it would appear that all of these materials were derived from the evaporation of formation water from the core material and do not represent solid phases actually present in the host formation. Calcite is present as a cementing matrix between the clastic grains, as coarse fragments of pyritiferous limestone and shell material, as finer grains of foraminifera, and as clay-size material. No aragonite or other carbonates were found.

The sand fraction is composed chiefly of quartz (many varieties and types: see detailed sand descriptions), chert, K-feldspars (microcline and sanidine), plagioclase, iron sulfides, and very minor heavy minerals. Magnetic minerals are notably absent from all samples. The grains are loosely-cemented to well-cemented with pyrite and calcite. The proportion of attached pyrite makes a slight inaccuracy in the weight of the specific gravity fractions.

The size distribution (figs. 1, 2, 3, 4), heterogeneity of quartz grains, relative absence of heavy minerals, and fossil content suggest that these are samples of a beach sand. The K-feldspars are maximum microcline and subordinate sanidine; orthoclase and adularia are scarce to absent. The sanidine is vitreous and fresh with inclusions of biotite, whereas the microcline is mostly weathered and partially altered to clay minerals (montmorillonite). Plagioclase includes the ranges from An_0 to approximately An_{45}; more calcic material may be present, but was not detected in this study. Pyrite is more abundant in the coarser grain sizes with marcasite increasing in abundance in the finer fractions.

Pyrite is invariably the matrix material other than calcite cementing the clastic grains. Some of the clinoptilolite is black and nearly opaque from included pyrite, and some clinoptilolite grains appear to be pyrite pseudomorphs.

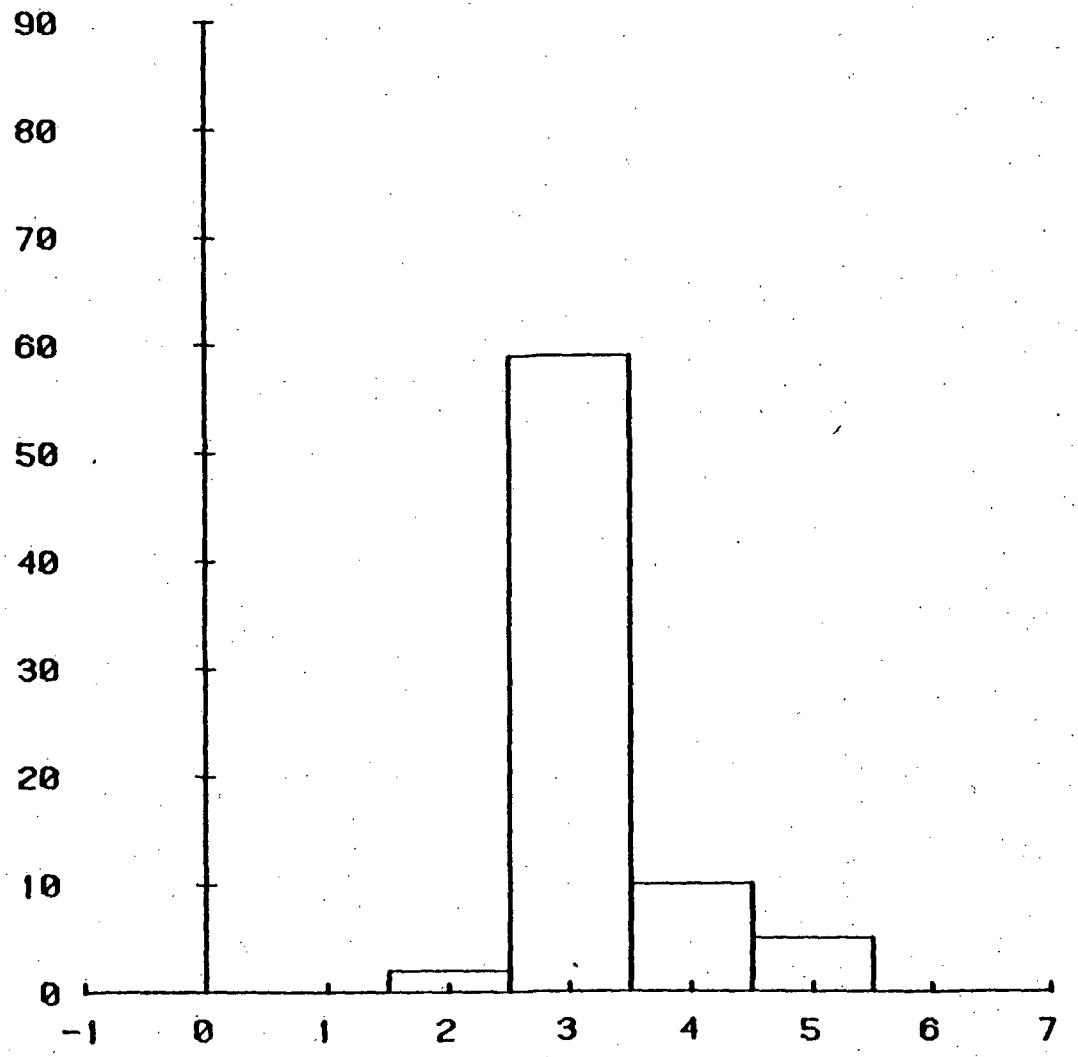

Figure 1. Sand size distribution of core material from USBM-2. 10 = +20, 2 = -20 to +40, 3 = -40 to +80, 4 = -80 to +120, and 5 = -120.

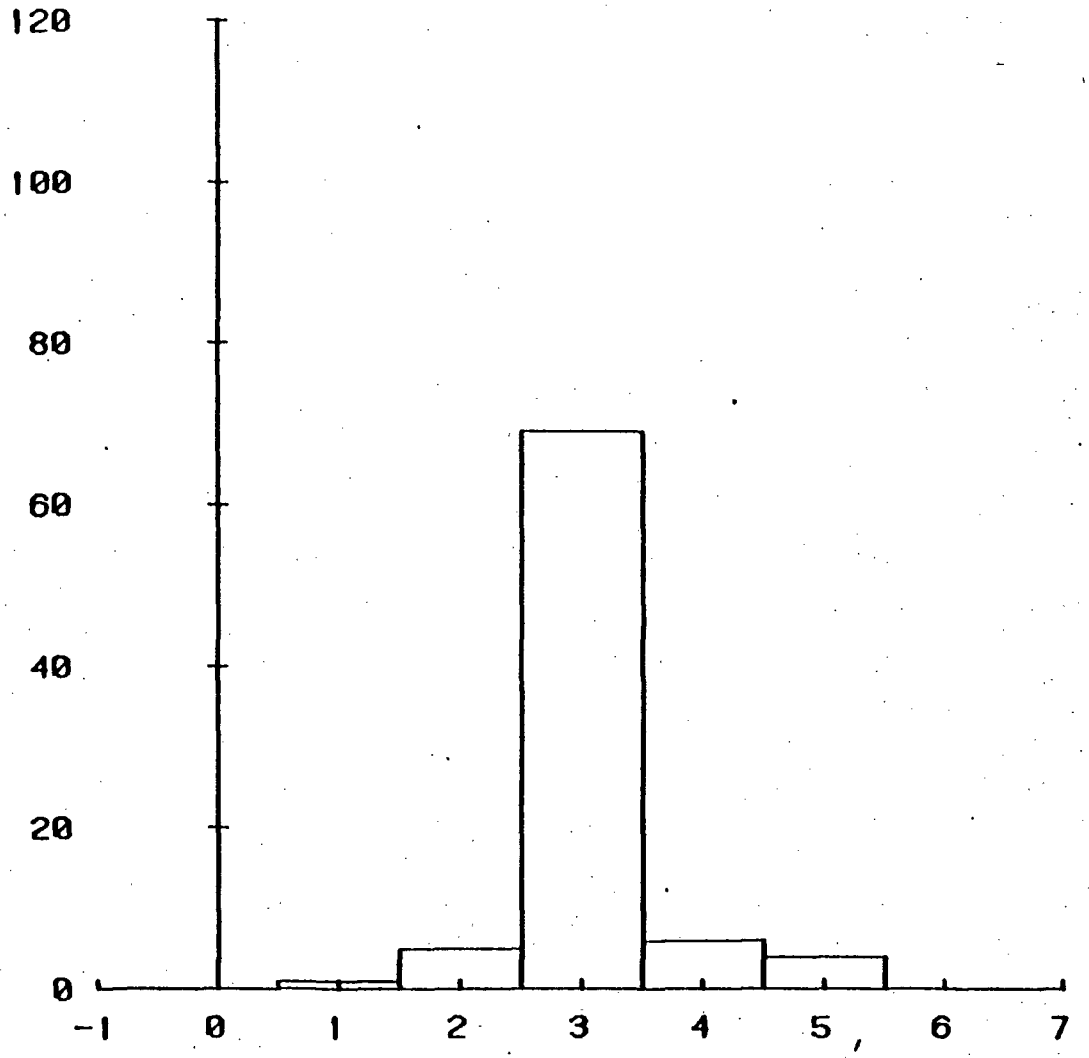

Figure 2. Sand size distribution of core material from USBM-4. 1 = +20, 2 = -20 to +40, 3 = -40 to +80, 4 = -80 to +120, and 5 = -120.

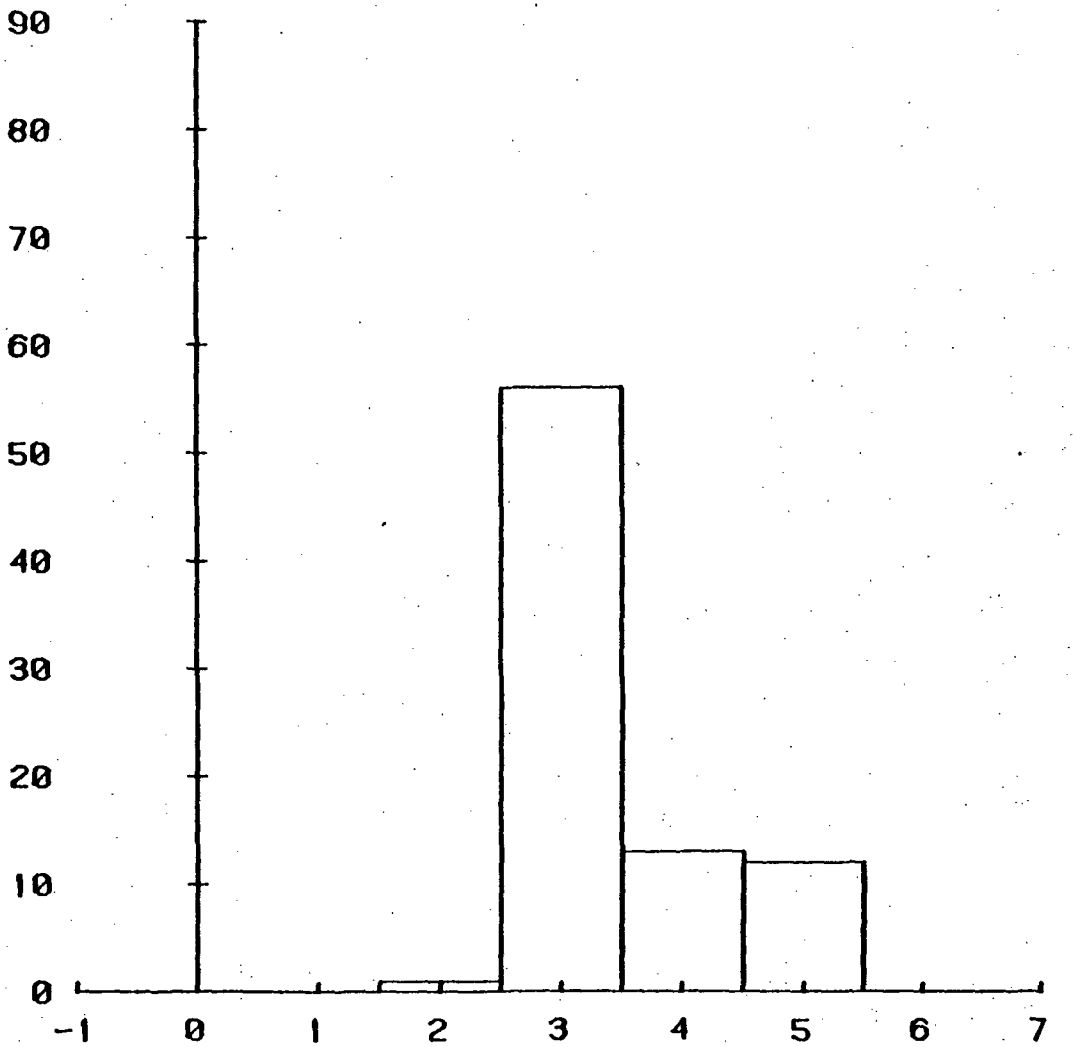

Figure 3. Sand size distribution of core material from USBM - 7. 1 = +20, 2 = -20 to +40, 3 = -40 to +80, 4 = -80 to +120, and 5 = -120.

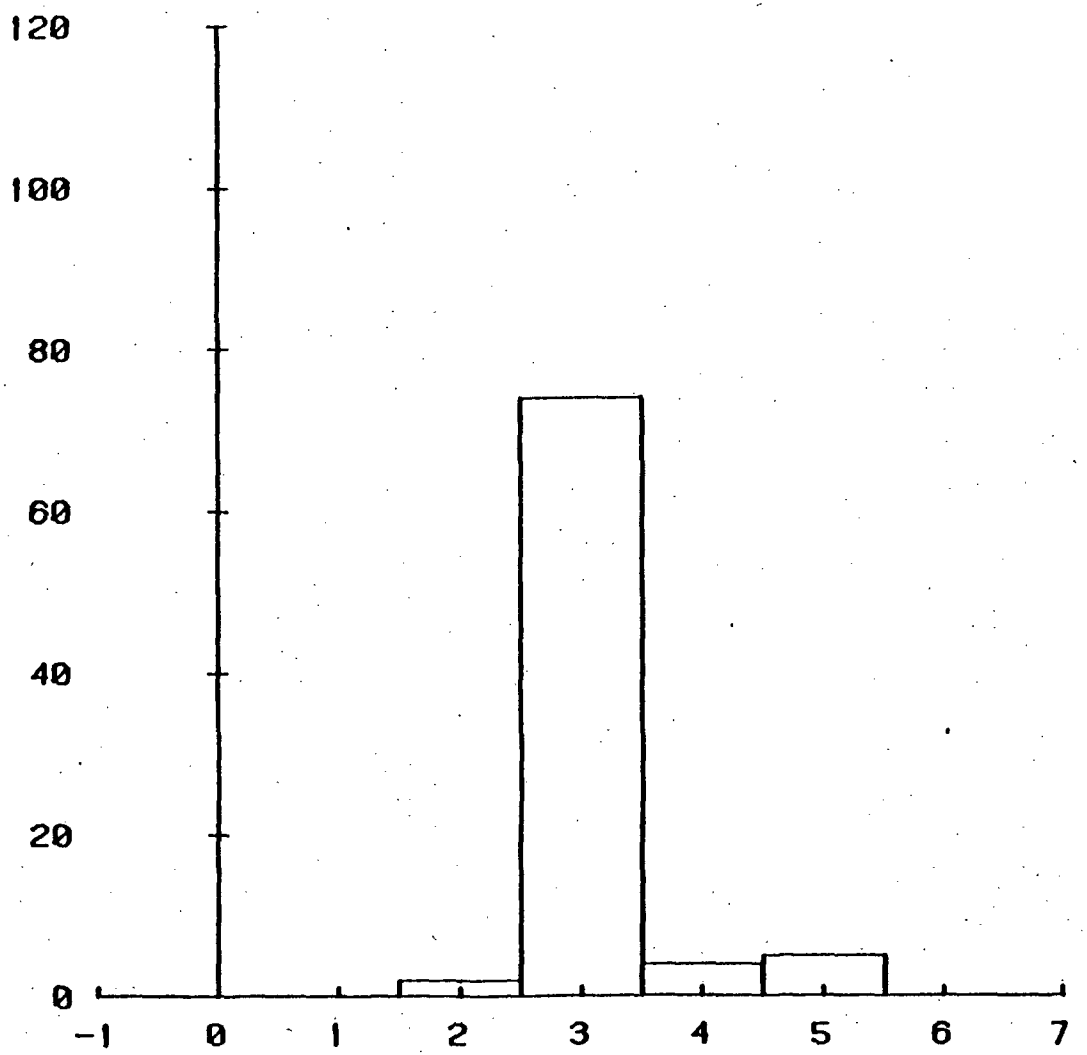

Figure 4. Sand size distribution of core material from USBM -8. 1 = +20, 2 = -20 to +40, 3 = -40 to +80, 4 = -80 to +120, and 5 = -120.

Detailed Sand Franction Descriptions

USBM-2

-20 +40 mesh. Has the same minerals, in general, as the -40 +80 mesh size (described below). Noteworthy are several subhedral to euhedral crystals of clinoptilolite colored black with inclusions of fine-grained pyrite.

-40 +80 mesh. This fraction, which makes up almost 70% of the whole sample, was studied in more detail than the other size fractions. It was separated, with heavy liquids, into the following components having the indicated specific gravities:

>2.85. Mostly marcasite with minor pyrite. A very small, weakly magnetic, fraction consists of rounded ilmenite grains coated with pyrite. There is no magnetite present. Heavy minerals are virtually absent from the total sand sample as they constitute only about five percent of this fraction (or less than 0.05% of the whole sample). The heavy minerals, in approximate order of abundance, are sphene, zircon, tourmaline (schorl; dravite), garnet (not identified), and biotite.

2.85 - 2.67. Mostly quartz and calcite with minor albite and very minor microcline.

2.67 - 2.62. Quartz, microcline, and albite. The quartz grains are predominantly angular to subangular, but some are well rounded. About one-third of the quartz present is in the form of chalcedony: mostly black and opaque, but some reddish brown and translucent. The feldspar is subangular and weathered.

2.62 - 2.57. Microcline, quartz, and very minor clinoptilolite. The microcline ranges from weathered to nearly fresh and from colorless, through white, to black from unidentified included material. Handpicked, fresh, colorless to white grains give an X-ray diffraction pattern of maximum microline:

a (Å)	8.579(2)		
b	12.964(2)		
c	7.218(1)		
α	90° 41(1)'	α*	90.35°
β	115° 54(1)'	β*	64.11°
γ	87° 44(1)'	γ*	92.20°
V (Å^3)	721.6(2)		

These dimensions indicate a composition of Or_{96-98}.

2.57 - 2.28. Almost entirely microcline with minor quartz as determined by optical examination. The feldspar is mostly weathered.

<2.28. Microcline, minor quartz, and clinoptilolite. The microcline in this fraction is chiefly white and considerably attacked by weathering. A portion of the microcline has the form of rounded white nodules; the X-ray diffraction pattern of this microcline exhibits broad peaks with weak intensities. However, no clay minerals nor other alteration products could be detected in this material. There is also a smaller amount of gray microcline present.

The clinoptilolite is present both as platy euhedral crystals, rosettes, and fine-grained massive material. The coarser crystals are black and nearly opaque from included pyrite. Designation as clinoptilolite is based on the thermal stability of the structure to temperatures up to 700°C in heating experiments. The clinoptilolite had the unit-cell dimensions:

a (Å)	17.70(1)
b	17.92(1)
c	7.416(3)
β	116° 23(3)'
V (A^3)	2107(2)

-80 +120 mesh. Separated into sp gr >2.85 (0.8 g; 2.5 wt.%) and sp gr <2.85 (31.2 g; 97.5 wt.%). The heavy fraction is composed of marcasite with subordinate pyrite. Heavy minerals are less than 5%. The light fraction is mostly quartz with calcite and minor microcline and albite.

-120 mesh. Separated into sp gr >2.85 (1.6 g; 7.6 wt.%) and sp gr <2.85 (19.4 g; 92.4 wt.%). Compositions of both fractions are similar to the -80 +120 mesh fractions above, but marcasite is relatively more abundant in the heavy fraction and calcite is more abundant in the light fraction in the finer mesh size.

USBM-4

-20 +40 mesh (whole fraction): Quartz, plagioclase, K-feldspar, pyrite, and clinoptilolite. Microcline is present as light gray nodules with inclusions of pyrite. About 15% of the total sand sample is composed of smoky quartz which is very dis- tinctive. It is most abundant in this mesh size and becomes scarcer as the mesh size decreases. It appears as subhedral crystals to angular fragments, is transparent, and colored light reddish brown. The color disappears after heating to 300°C for several hours. Some of the angular fragments are 1.5 mm in greatest dimension, but the subhedral to euhedral crystals are as small as 0.45 mm in diameter so that there is a fair range in size. The smoky color has been attributed to free Si formed by natural irradiation. This may well have been the cause of the color of this smoky quartz at the original source, but it is unlikely in-situ as there is a great variety of associated quartz showing no such effects. The source of this quartz may be quite local, however, for there is very little evidence of rounding, abrasion, or other effects of transport. Smoky quartz is most abundant in this sample. There is less than ten percent in sample USBM-7 and only an occasional grain can be found in sample USBM-8.

-4 +80 mesh. As shown in table 1, this fraction makes up nearly 70% of the whole sample. It was separated with heavy liquids into the various specific gravity fractions discussed below.

>3.31. Pyrite, clinoptilolite, and marcasite. There is more of the zeolite in this fraction than in the lighter fractions due to the included or replacing pyrite. Heavy minerals which are mostly yellow sphene, garnet, and zircon are present as minor constituents (less than ten percent of this fraction).

3.31 - 2.85. Quartz (with attached pyrite), plagioclase, K-feldspar, pyrite, clinoptilolite, marcasite, and micas. Less than two percent of this fraction is composed of white, frosted, prismatic grains of fluorapatite (ω - 1.634). Minor heavy minerals: sphene, tourmaline, and garnet.

2.85 - 2.67. Quartz, plagioclase, K-feldspar, minor pyrite, marcasite, and trace of muscovite. Much of the plagioclase is andesine (approximately An_{45}) and occurs as prismatic to tabular subhedral clasts showing etching and other effects of solution. There are minor, but distinctive, green clasts of pyritiferous schist composed of quartz, plagioclase, green muscovite (chromiferous?), and chlorite.

2.67 - 2.62. Constitutes over 50% of the whole sample. Quartz, K-feldspar, and plagioclase. There is a wide variety of quartz present. It varies from clear to opaque; colorless to black; coarsely crystalline to compact; fresh and angular to rounded and frosted. There is a major amount of deep brownish-black chert present.

2.62 - 2.57. K-feldspar (microcline, sanidine), plagioclase, quartz, and trace of pyrite. Some of the microcline in this fraction is nearly black; some is light gray with small spherules of pyrite. The microcline appears as block subangular to subrounded clasts. Sanidine is colorless, angular, subhedral, with some inclusions of biotite.

2.57 - 2.28. Microcline, quartz.

<2.28. Weatherered microcline with minor plagioclase, pyrite, and clinoptilolite.

-80 +120 mesh (whole fraction). Mostly quartz with subordinate K-feldspar, plagioclase, and very minor pyrite and muscovite.

-120 mesh (whole fraction). Quartz with K feldspar and plagioclase.

USBM-7

This sample is closely similar in most respects to sample USBM-4 and, except for some details, only a generalized description is given here.

-20 +40 mesh (whole fraction). Quartz, plagioclase, K-feldspar, pyrite, and clinoptilolite.

-40 +80 mesh (specific gravity fractions).

>3.31. Pyrite, marcasite, and minor sphene, garnet, and trace of zircon. Heavy minerals are less than ten percent of this and the following fraction.

3.31 - 2.85. Pyrite, marcasite, quartz (with attached pyrite), clinoptilolite (with pyrite), and minor fluorapatite, sphene, tourmaline, and garnet.

2.85 - 2.67. Quartz, plagioclase, pyrite, and minor mica (chiefly muscovite).

2.67 - 2.62. Chiefly quartz with minor plagioclase.

2.62 - 2.57. Quartz, K-feldspar, and plagioclase.

2.57 - 2.28. Microcline with minor quartz.

<2.28. Microcline, some plagioclase (mostly weathered material), minor pyrite, and a trace of clinoptilolite.

-80 +120 (whole fraction). Quartz, plagioclase, K-feldspar with minor pyrite and marcasite.

-120 (whole fraction). Quartz with K-feldspar, plagioclase, marcasite, pyrite, and very minor clinoptilolite. Marcasite predominates over pyrite in the finest size material.

USBM-8

Similar to the preceding samples. There is noticeably less of the smoky quartz in this sample, however, and there is a bluish-green pigment in part of the clay matrix. An X-ray diffraction pattern of this material showed only montmorillonite and quartz and the nature of the pigment itself is still not known. It is a very minor constituent, but distinctive.

-20 +40 mesh (whole fraction). Quartz, plagioclase, and K-feldspar (in about equal amounts and both fairly well weathered), minor pyrite, and clinoptilolite (with included pyrite).

-40 +80 mesh (specific gravity fractions).

>3.31. Pyrite and marcasite. Very minor heavy minerals are sphene, garnet, zircon, and tourmaline.

3.31 - 2.85. Pyrite, marcasite, plagioclase (with pyrite), and quartz (with pyrite). Very minor heavy minerals are sphene, tourmaline, and garnet, and fluorapatite.

2.85 - 2.67. Quartz, plagioclase, minor muscovite, pyrite.

2.67 - 2.62. Quartz with subordinate plagioclase and very minor muscovite.

2.62 - 2.57. K-feldspar and quartz, minor plagioclase.

2.57 - 2.28. Microcline with very minor quartz and clinoptilolite.

<2.28. Microcline, minor quartz, and clinoptilolite. The blue-green pigmenting material is concentrated in this fraction.

-80 +20 mesh (whole fraction). Quartz, plagioclase and K-feldspar, minor pyrite, and trace of clinoptilolite.

-120 mesh (whole fraction). Same as above.

USBM-2a

Clay shale. Greenish-gray (5GY 6/1), silty, calcareous (calcite) clay transected by a thin (5 mm) pyritiferous calcareous (calcite) seam. The clay minerals are composed predominantly of Ca-montmorillonite with subordinate, and randomly interstratified, chlorite and illite (hydrous mica). The silt fraction is mostly quartz, microcline, pyrite, and minor albite. A very small amount of the quartz, pyrite, and microcline are also present in the clay-sized fraction. No clinoptilolite, nor marcasite were found in the sample.

Chemistry of Formation Waters:

Figure 5 shows the location of wells studied. Some distant monitoring wells sampled to obtain a better understanding of the regional variations of the formation water chemistry are not shown. Prior to the introduction of lixiviant into the formation, a suite of samples was collected from the USBM test wells, a company production well, and two outlying company monitoring wells. Pumps were mounted in the wells and were used to obtain the water samples. The pumps all had been in place for several days before any samples were collected. Approximately five well volumes of water were pumped prior to the collection of any samples. The samples were all collected through a small bypass which diverted some of the flow from the well to a tee which allowed the water to be passed through a filter and/or a flow-through cell for measuring Eh and pH (fig. 6).

At each sampling of the well, a series of four samples were collected. The first sample was a 500-mL unfiltered, unacidified sample. Three 500-mL samples which had been filtered through a 0.1 μm membrane filter were then collected. One of the samples was acidified with 2 mL of analyzed 6 normal nitric acid. The other two samples were not acidified. One of the filtered samples was used for field analyses and the remaining three were kept for laboratory analyses. The samples were collected in polyethylene bottles and sealed with screw caps with a polyethylene cone fitting which provides an air-tight seal.

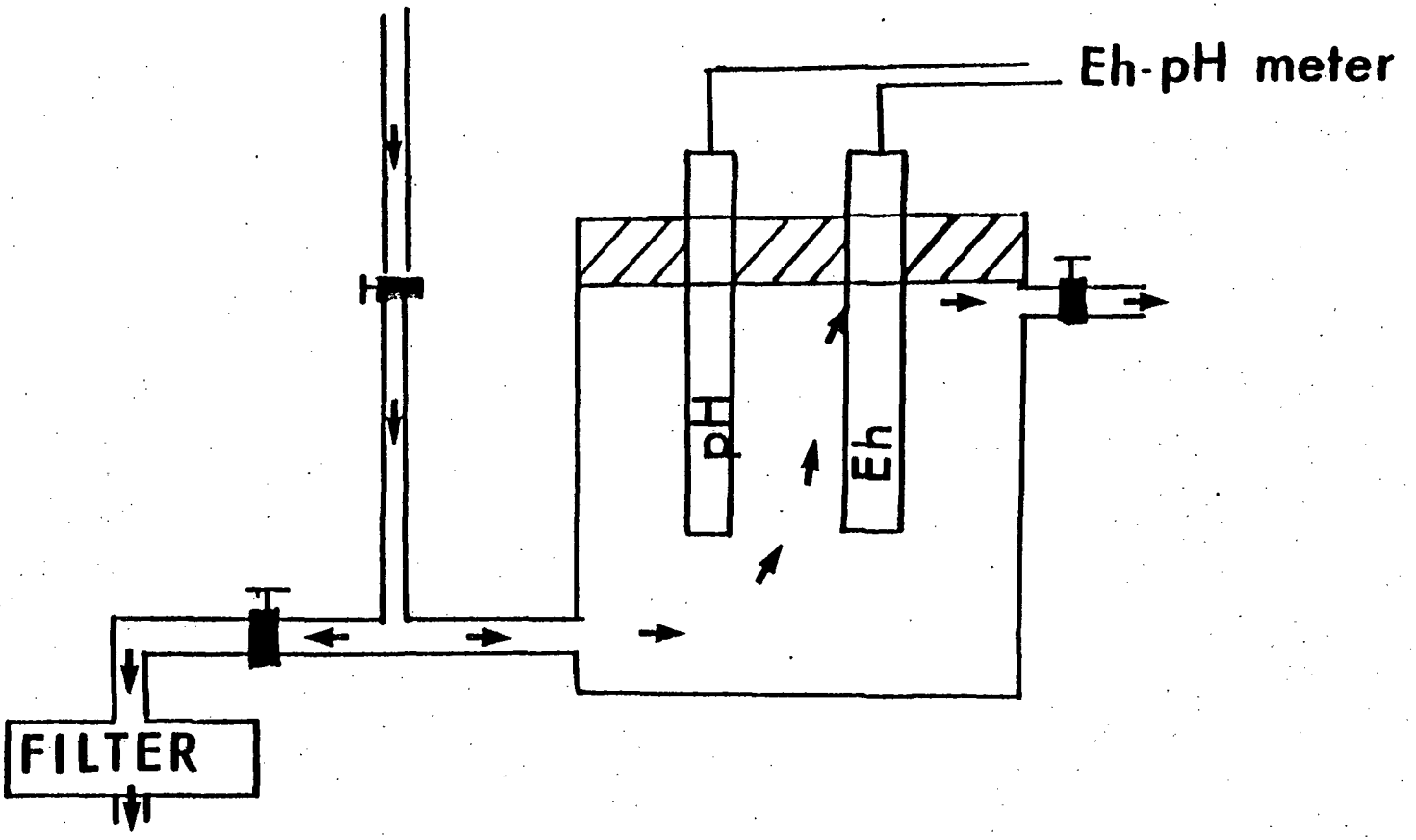

Figure 6. Schematic of the flow through cell used to obtain pH and Eh measurements as well as filtered samples.

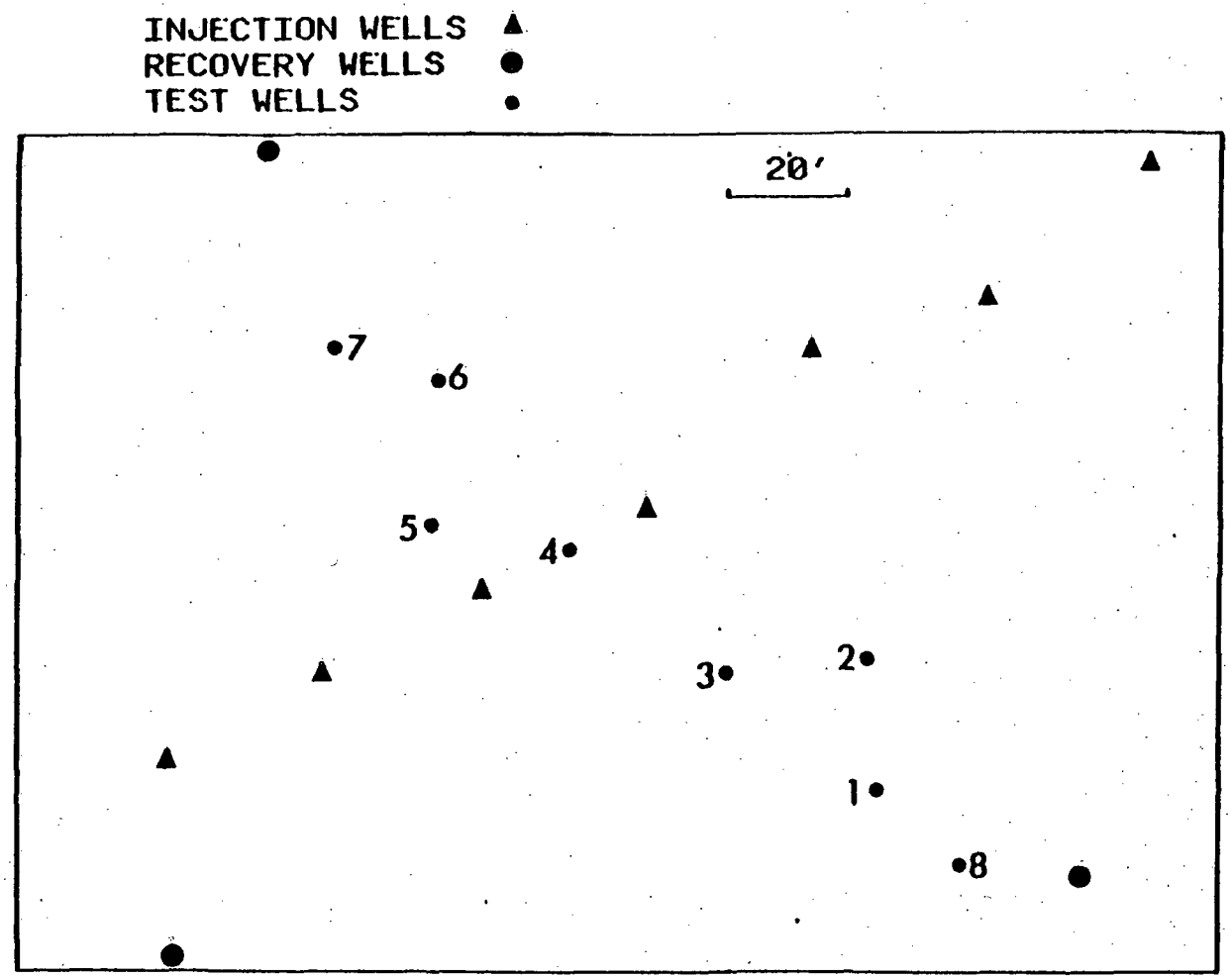

Figure 5. Location map for leaching experiment.

In addition to the pumped samples, formation waters were also obtained using a gas-tight downhole sampler that had been designed for sampling geothermal fluids. The downhole sampler would capture approximately 500-mL samples which then transferred through gas tight fittings into an evacuated (10^{-2} torr) 500-mL glass bottle leaving a small (10 mL) headspace. The glass bottle was then sealed by means of O-ring seals while still connected to the sampler. The samples were then retained for laboratory analyses of the dissolved gas contents of the water. In addition to the downhole water samples, a series of downhole temperature measurements were made using a maximum reading thermometer. The downhole temperature measurements were conducted at night while the air temperature was less than 15°C.

As the pumped samples were collected a series of field measurements were conducted to measure fluid properties and to obtain concentration data on fugitive constituents which could not be preserved by the sampling procedures (Eh, pH, and HCO_3). Field analytical methods for constituents of interest to in-situ leach operations (Na, K, and Ca) were also tested.

The Eh and pH of the formation waters were measured simultaneously in a flow-through cell (fig. 6). A portion of the well flow that was diverted into the bypass tube was used to flush the plastic cell with four to five volumes of effluent (one cell volume is approximately 200 mL). The combination Eh and combination pH electrodes were then inserted into the plastic cell being careful to exclude air bubbles.

The flow through the plastic cell was reduced to approximately 20 mL/min. When the emf of the combination Eh electrode had stabilized (±10 mv), usually after 30 to 45 minutes, the Eh and pH values were recorded. In contrast to the Eh value, the pH value usually stabilized in a few minutes although continuous readings were taken until the Eh electrode values had stabilized. The temperature of the fluid in the cell was also measured with a mercury thermometer which had been previously calibrated against a platinum resistance thermometer. The combination Eh electrode was standardized with Zobell's solution and was found to be stable enough (±3 to 5 mv) that usually only one standardization per day was necessary. Before and after the pH measurements the pH electrode was standardized using pH 4, 7, and 9 buffers.

The bicarbonate concentration was determined in the field using the following titration procedure. A 100-mL aliquot of filtered formation water was placed into a beaker along with a magnetic stirring bar and 3 drops of methyl purple indicator. A combination pH electrode standardized using pH, 4, 7, and 9 buffers was transferred into the beaker. The solution was then titrated with standardized 0.05 normal sulfuric acid. Pairs of pH readings and acid volumes were recorded until the indicator turned gray at a pH of 5.1. A minimum of three pairs of acid volumes and pH values were then obtained between pH 5 and pH 4. The amount of bicarbonate was then computed from a least-squares regression of the entire titration curve which was used to calculate the end point exactly (Barnes, 1964). This method of

determining the end point is far more precise than the usual method of using a fixed end point of 4.5. The standardization of the combination pH electrode was again checked along with temperature at the conclusion of the titration. Any shifts were then used in the computation of the end point as required.

The increase in the Na and K concentrations of the lixiviant (usually formation water plus $(NH_4)_2CO_3$ with or without oxidant) during the leaching process are good indicators of the degree of ion-exchange occurring between the lixiviant and the formation. Hence a field analytic method for measuring Na and K concentrations in groundwater and lixiviant could prove to be a useful tool for on site monitoring of the performance of an in-situ leaching operation. Correspondingly, we tested the behavior of ion-selective electrodes specific for Na and K as possible field or on-stream analytical methods.

The K concentration was determined by taking a 100-mL aliquot of filtered formation water and adjusting the ionic strength by adding 2 mL of 6 molar NaCl solution. The K electrode and a double junction reference electrode were then immersed in the solution and the emf allowed to stabilize. The emf value was then recorded and the concentration determined from a calibration curve determined from a set of 3 to 4 standards. A similar procedure was followed for Na except that the ionic strength was adjusted with 3 mL of 4 molar KCl solution.

The Ca content of the formation water is of concern because of difficulties arising from precipitation of calcite during the leach operations. Radium and uranium co-precipitates with calcite resulting in a radioactive low level waste which must be disposed of. Calcium also interferes with the extraction of the uranium from the lixiviant. Hence, the ability to monitor Ca is of practical significance.

We tried two procedures as field analytical methods. The first was a standard titration with EDTA and the second was using a Ca ion-selective electrode. Due to difficulties with direct measurement, we had to use the electrode with an EDTA titration to improve the precision. However, it soon became apparent that the regular EDTA titration was far more reliable and use of the electrode was abandoned.

The three 500-mL samples which were taken back to the laboratory were analyzed by standard methods for the major constituents. Several methods were employed to check for trace element contents. One method was to evaporate to dryness 100 mL of sample and to do a quantitative analysis of the evaporate by emission spectroscopy. The second, more novel, method employed emission spectroscopy with an inductively coupled plasma. Table 2 shows which methods were employed to analyze which constituent.

Table 2. Methods employed for laboratory analyses of samples

Constituent	Atomic Absorp-	Spectrophotometric	Gravimetric	Direct potentiometry	Titration	Plasma emission spectroscopy	Emission spectroscopy
SiO_2	X	X				X	X
Fe	X	X					X
Ca	X					X	X
Mg	X						X
Na	X						X
K	X						X
Li	X					X	X
Al	X					X	X
As							X
Ba							X
Cd							X
Cr							X
Cu							X
Pb							X
Mn							X
Hg							X
Mo							X
Se							X
Ag							X
V							X
Zn							X
Ur		X				X	X
NH_4				X			
SO_4		X	X				
Cl				X	X		
F				X			
PO_4		X					
B		X				X	X
H_2S		X	X				
CO_3		X	X				
HCO_3					X		

The samples collected by the downhole gas-tight sampler were analyzed for the various gaseous components as follows. The major residual gases (gases in the headspace above the sample) were analyzed with a gas chromatograph equipped with a Carle Thermistor Detector and 6-foot Poropak Q and 20-foot molecular sieve 5A columns in series held at 27°C. Helium carrier gas at 60 psi inlet pressure was used for analysis of O_2, Ar, N_2, and CH_4 while argon carrier gas at 50 psi inlet pressure was used for He and H_2. Hydrocarbon gases were analyzed with a Hewlett Packard flame ionization gas chromatograph. Dual 6-foot Poropak Q columns were used with helium carrier gas at an inlet pressure of 60 psi, and the analysis temperature programmed from 30°C to 150°C.

Analytical Results:

The baseline data for the major constituents are summarized in table 3 while the analytical data for the dissolved gases are contained in table 4.

Well #602 was sampled and analyzed by the U.S. Geological Survey, the Texas Water Quality Board (TWQB), and the operating company. A detailed comparison of the three sets of analyses are listed in table 5. The data differ significantly only in uranium, the pH and HCO_3. For pH and HCO_3 this is because our measurements were done in the field while the others were done on stored samples. CO_2 will escape from the stored samples, causing precipitation of calcite and thus lowering the HCO_3 content and increasing the pH. The filtered unacidified sample taken for laboratory analyses had a pH of 7.82 when measured in the laboratory three weeks later, compared to a field pH of 6.98.

Table 3. Baseline data for groundwater. All values are in mg/L except for Eh (mv), pH and T°C.

	USBM 1	USBM 3	USBM 4	USBM 7	USBM 8	USBM 6*	Company #602
Eh	-131	-119	-98	-70	-140	-85	-100
pH	6.90	7.01	6.97	7.18	6.95	7.11	6.98
T	24.5	24.5	25.4	24.8	25.4	24.5	25.4
Na	153	125	165	130	128	123	125.0
K	11.9	12.0	10.9	13.8	11.1	17	11.4
Ca	48.6	59.3	57.5	57.0	53.0	56	55.0
Mg	5.4	5.9	5.8	5.1	5.7	5	5.8
Al	.003	.001	.003	.003	.003	—	.003
Fe	.12	.11	.12	.10	.11	—	.12
Li	.035	.035	.045	.040	.040	—	.04
SiO_2	38	35	32	31	35	—	37.0
U	.01	.11	.10	.09	.0006	—	.50
NH_3	.1	.1	.1	.1	.1	—	.1
SO_4	65	72	100	114	76	—	81.0
Cl	94	76	177	75	76	—	75.0
F	.55	.60	.50	.55	.60	—	.55
PO_4	.05	.05	.05	.05	.05	—	.05
HCO_3	328	341	326	354	337	—	337
B	1.1	1.0	1.1	.8	1.23	—	1.2
As	-	-	-	-	-	—	.02
Cd	-	-	-	-	-	—	N.D.
Cu	-	-	-	-	-	—	.03
Pb	-	-	-	-	-	—	.03
Mn	-	-	-	-	-	—	.04
Mo	-	-	-	-	-	—	.50
V	-	-	-	-	-	—	.03
Zn	-	-	-	-	-	—	.03
Cr	-	-	-	-	-	—	N.D.
Hg	-	-	-	-	-	—	N.D.
Se	-	-	-	-	-	—	N.D.
Ag	-	-	-	-	-	—	N.D.

* Field Analyses only

Table 4. Gas Analyses for downhole sampler.
Values reported as mg/L dissolved in water.

	USBM 1	USBM 3	USBM 7	Company 106	Company 115	USBM 3*
He	0.03	0.03	0.03	0.03	0.03	0.03
H_2	.03	.03	.03	.03	.03	.03
Ar	.03	.056	.102	.125	1.804	.046
O_2	.03	.03	.03	.03	.03	.03
N_2	26.44	3.684	3.978	6.481	57.21	3.581
CH_4	.905	.915	--	--	--	--
C_2H_6	.002	.002	--	--	--	--
Propane	.002	.002	--	--	--	--
NH_3	.1	.1	.1	.1	.1	high
H_2S	.2	.3	N.D.	N.D.	1.6	.2

*Samples collected after the arrival of the lixiviant

The data in tables 3 and 4 were used to calculate mineral saturation through the use of the computer programs SOLMNEQ (Kharaka and Barnes, 1973) and WATEQ (Truesdell and Jones, 1974). The waters are in equilibrium with minerals of the host formation with but few exceptions. The most notable is pyrite, which is extremely supersaturated, with significant iron and hydrogen sulfide present in the formation water. The mineralogic evidence suggests that clinoptilolite is forming in the sands with pyrite but there are no thermodynamic data available to check this observation with the solution chemistry.

A most interesting result of the baseline study is the apparent indication that the orebody is currently forming. The strongest pieces of evidence are the strong Eh gradient across the deposit and the very rapid decrease in the uranium content of the water across the orebody. The pH of the formation waters showed no apparent correlation with the orebody; however, where data were available there was a strong correlation between calcite content of the well and the pH of the formation water removed from the well. The Eh gradient present in the orebody is apparently related to the migration of H_2S from deeper oil field brines which is subsequently oxidized to sulfate by the inflow of oxygenated groundwater. These phenomena are of significance to the in-situ leach operations. On the oxidizing side of the oxidation-reduction front uranium can be solubilized more readily with less or no additional oxidant, while on the reducing side significantly larger quantities of oxidant will be required to obtain the same uranium concentrations in solution.

Table 5. Comparison of Analyses for Baseline Data of Well #602 with those of the Texas Water Quality Board and the Operating Company

Element or Measurement	USGS	TWQB	Company
Eh (mv)	-100.0	—	—
pH	6.93 0.3	8.1	7.3
T°C	25.4	—	—
SiO_2	37	—	—
Fe	.12	—	—
Ca	55	61	51
Mg	5.8	6.1	6
Na	125	120	135
K	11.4	—	—
Li	.04	—	—
Al	.003	—	—
As	.02	.01	.02
Ba	.1	.5	.5
Cd	N.D.	.01	.002
Cr	N.D.	.01	.01
Cu	.03	.05	.02
Pb	.03	.05	.02
Mn	.04	.1	.06
Hg	N.D	.0005	.0001
Mo	.5	.5	.55
Se	N.D.	.002	.005
Ag	N.D.	—	.002
V	.02	—	.018
Zn	.03	.1	.03
U	.50	1.3	.53
NH_3	.1	.1	.1
SO_4	81	—	72
Cl	75	—	78
F	.55	—	—
PO_4	.05	—	—
B	1.20	—	.6
H_2S	.30	—	—
HCO_3	337	—	280

LEACHING PHASE

Lixiviant Chemistry Versus Time:

Methods used to sample the groundwater prior to the injection of the lixiviant were also employed to sample and preserve the lixiviant samples. The only difference in procedure was to cease field titrations for HCO_3 after the lixiviant had arrived and not to acidify the high carbonate samples with nitric acid. The analytical methods were all the same as used previously; however, the standards used in the analyses were made so as to have the same general matrix as the lixiviant.

The lixiviant was manufactured by dissolving gaseous ammonia and carbon dioxide in the groundwater. The lixiviant was put into the formation at the injection wells near USBM-4. The following wells were sampled daily or more frequently as conditions warranted: USBM-1, USBM-3, USBM-4, AND USBM-7. The data obtained are summarized in tables 6, 7, 8, and 9.

Table 6. Summary of Chemical Analyses for USBM-1

	Day	Date	T°C	pH	HCO_3	Na	K	Ca	Mg	SiO_2	CO_3^{2-}	NH_4	SO_4^{2-}	Cl^-	U
2	0	3-19	--	6.90	312	165	12.8	41.5	5.10	--	--	<0.1	--	94	0.01
11	1	3-20	26.0	7.30	341	150	11.5	47.5	5.45	--	--	<0.1	69	92	--
16	2	3-21	26.0	7.20	308	148	11.6	51.0	5.64	--	--	<0.1	--	--	--
20	3	3-22	25.9	6.96	341	148	11.8	54.5	5.45	--	--	<0.1	--	85	--
21	4	3-23	--	7.19	363	143	11.6	53.5	5.75	--	--	<0.1	--	--	--
31	6	3-25	28.0	8.00	400	143	11.6	54.0	5.90	39	--	<0.1	46	80	0.02
39	9	3-28	28.0	7.50	392	140	11.7	54.0	5.85	38	--	<0.1	59	--	--
40	10	3-29	28.0	7.01	348	139	11.6	54.0	5.90	40	--	<0.1	--	80	--
48	12	3-31	27.5	7.23	345	139	11.7	55.0	5.85	--	--	<0.1	--	78	--
56	14	4-2	--	7.44	367	138	11.6	91.5	6.00	38	--	<0.1	--	--	--
62	15	4-3	26.0	7.75	363	137	11.6	56.0	6.10	--	--	<0.1	--	76	--
65	16	4-4	26.0	7.17	358	136	11.9	54.0	5.95	--	--	<0.1	66	--	--
69	17	4-5	24.0	7.50	--	135	--	--	5.90	--	--	<0.1	--	--	0.8
72	18	4-6	24.5	7.31	334	139	11.5	76.3	6.05	--	--	<0.1	--	84	--
77	19	4-7	24.0	6.98	334	134	10	31.0	7.00	36	--	<0.1	66	--	--
81	20	4-8	24.0	6.96	341	126	10	30.6	7.20	--	--	<0.1	--	82	--
89	22	4-10	24.0	6.77	479	164	12	30.8	9.20	--	--	<0.1	--	91	--
95	23	4-11	24.0	9.05	--	126	37	18.8	17.8	40	900	510	64	--	5.0
99	23.5	4-11	28.0	9.42	--	170	144	1.5	24.2	--	1680	953	--	--	19.5
101	24	4-12	28.0	9.21	--	--	318	1.2	26.4	--	2760	1566	--	112	--
105	25	4-13	28.0	9.39	--	194	362	1.1	22.8	--	4980	2827	71	--	--
109	26	4-14	28.0	9.34	--	179	368	1.3	24.4	35	6540	3712	--	--	--
113	27	4-15	28.0	9.31	--	167	368	1.1	22.8	--	6480	3678	91	131	2.3
119	29	4-17	28.0	9.34	--	164	319	1.2	22.7	--	5940	3372	--	129	--
124	31	4-19	28.0	9.16	--	--	283	1.1	26.1	34	5880	3338	83	124	1.5
129	33	4-21	28.0	9.04	--	138	167	1.6	10.3	33	2760	1566	--	116	--
133	35	4-23	28.0	9.00	--	102	116	3.8	8.8	--	1320	749	71	110	18.5
135	36	4-24	28.0	9.58	--	167	197	1.2	29.5	23	2640	1498	--	--	>5
142	37	4-25	28.2	9.28	--	298	270	1.2	29.4	18	4020	2282	--	121	3.3
143	38	4-26	29.0	9.49	--	126	--	1.0	30.4	16	6780	3849	--	127	>5
149	39	4-27	30.0	9.30	--	148	--	2.6	32.4	10	8461	4802	59	139	2.9
155	40	4-28	30.0	9.08	--	--	187	1.8	20.4	--	7201	4087	--	134	--
157	41	4-29	30.0	9.23	--	--	110	2.6	14.5	--	4740	2690	--	124	--
161	42	4-30	29.5	9.08	--	211	78	3.0	10.5	--	3780	2145	--	--	0.5
165	42.5	4-30	29.5	9.30	--	116	63	2.5	11.4	--	4380	2486	86	--	--
168	43	5-1	29.0	9.50	--	273	71	2.3	12.5	--	4980	2827	--	120	--
171	43.5	5-1	30.0	9.60	--	282	70	2.3	13.0	--	5340	3031	--	--	--
173	44	5-2	29.0	9.71	--	283	76	2.2	11.8	11	5460	3099	--	--	1.7
178	44.5	5-2	30.0	9.30	--	270	82	1.9	11.1	--	5400	3065	114	--	--
179	45	5-3	29.0	9.50	--	294	88	2.3	10.7	--	5280	2997	--	126	--
184	45.5	5-3	29.5	--	--	134	88	2.1	10.6	--	5220	2963	--	--	--
185	46	5-4	29.0	9.50	--	147	86	2.4	10.4	--	4980	2827	--	--	--
190	46.5	5-4	29.5	9.50	--	134	87	2.3	12.1	--	4860	2759	146	--	--
191	47	5-5	29.0	9.30	--	148	93	2.8	11.2	12	5220	2963	--	122	1.0
194	47.5	5-5	29.5	9.40	--	278	92	2.2	11.7	--	5160	2929	--	--	--
195	48	5-6	30.0	9.30	--	267	94	2.3	12.9	--	5160	2929	--	--	--
210	50	5-8	30.0	9.50	--	233	120	2.4	14.4	--	5520	3133	167	123	--
216	51	5-9	29.5	9.40	--	130	121	2.5	14.7	--	5220	2963	--	--	--
217	51.5	5-9	29.0	9.50	--	280	127	2.2	15.1	--	5400	3065	107	--	1.3
222	52	5-10	29.0	9.50	--	133	136	2.1	14.5	12	5580	3167	--	--	--
223	52.5	5-10	29.0	9.30	--	278	138	1.8	13.2	--	5580	3167	231	--	--
228	53	5-11	29.0	9.50	--	282	147	2.2	14.2	8	5520	3133	--	122	--
229	53	5-12	29.0	9.40	--	290	160	2.3	15.7	--	5700	3235	--	--	--
234	53.5	5-12	29.0	9.40	--	288	167	1.7	15.4	8	5820	3304	--	--	--
235	54	5-13	29.0	9.50	--	282	172	1.4	14.6	--	6000	3406	223	--	--
302	55	5-14	--	--	--	237	130	--	--	--	--	--	--	--	0.7
303	56	5-15	--	--	--	277	120	1.8	10.6	--	4620	2622	114	120	--
308	57	5-16	--	--	--	--	117	2.3	11.3	--	4680	2656	--	--	--
309	58	5-17	--	--	--	--	118	2.3	13.7	--	4800	2725	287	--	--
314	59	5-18	--	--	--	246	118	2.1	14.0	8	4800	2725	223	120	0.8

Table 7. Summary of Chemical Analyses for USUM-1

	Day	Date	T°C	pH	HCO_3	Na	K	Ca	Mg	SiO_2	CO_3^{2-}	NH_4	SO_4^{2-}	Cl^-	U
4	0	3-19	--	7.20	312	120	13.7	65.5	5.8	45	--	<0.1	--	76	0.11
14	2	3-21	--	7.02	399	120	12.4	57.0	5.7	--	--	<0.1	41	--	--
24	4	3-23	26.0	6.98	341	130	12.0	32.5	6.3	--	--	<0.1	--	74	--
32	6	3-25	28.0	6.85	341	129	11.6	59.0	5.8	38	--	<0.1	71	98	--
38	8	3-26	26.0	7.10	341	129	11.3	58.0	5.9	--	--	<0.1	--	76	--
41	10	3-29	27.5	7.03	356	130	11.3	58.0	6.0	35	--	<0.1	--	--	--
47	12	3-31	27.5	7.30	341	130	11.6	58.0	6.0	--	--	<0.1	60	78	--
53	13	4-1	26.0	7.39	319	131	12.2	59.5	6.2	--	--	<0.1	--	--	--
57	14	4-2	26.0	7.43	363	147	12.8	64.0	7.0	35	--	<0.1	--	85	--
61	15	4-3	24.0	9.54	--	276	138	1.0	12.2	30	1800	1022	69	--	--
66	16	4-4	26.0	9.35	--	246	205	1.0	11.5	29	3060	1737	--	17	--
70	17	4-5	24.0	9.38	--	252	237	1.0	13.2	29	4861	2759	--	--	5.0
75	18	4-6	24.0	9.71	--	292	230	4.0	15.5	--	6301	3577	89	130	--
78	19	4-7	24.5	9.41	--	212	252	0.4	14.1	26	7561	4292	86	133	--
82	20	4-8	25.0	9.71	--	237	193	0.4	21.2	--	7621	4326	--	--	--
85	21	4-9	25.0	9.58	--	245	197	0.2	17.3	--	5941	3372	--	126	--
90	22	4-10	25.0	9.47	--	287	180	0.4	19.7	28	5101	2895	--	--	--
96	23	4-11	25.0	9.47	--	338	210	0.4	22.0	26	5521	3134	97	123	5.0
102	24	4-12	25.0	9.35	--	350	252	0.5	29.5	19	7261	4122	--	134	5.0
110	26	4-14	29.0	9.61	--	363	318	0.2	24.7	16	9301	5280	100	141	3.8
117	27	4-16	29.0	9.43	--	266	332	0.1	22.9	11	9661	5484	--	145	2.7
120	28	4-17	29.0	9.80	--	247	344	0.4	23.8	--	9781	5552	86	142	2.5
125	30	4-19	29.0	9.40	--	220	288	0.4	18.8	10	9901	5620	--	--	0.9
128	32	4-21	30.0	9.18	--	--	350	0.8	18.4	18	7621	4326	93	135	>5
132	34	4-23	29.0	9.2	--	272	206	3.1	12.3	--	4801	2725	--	--	--
136	35	4-24	29.0	8.42	--	261	136	3.4	10.0	17	1980	1124	43	--	4.1
141	36	4-25	28.0	8.55	--	238	126	8.8	10.2	--	9721	5518	--	--	--
144	37	4-26	28.0	9.28	--	243	137	3.3	21.1	17	2220	1260	--	113	5.0
148	38	4-27	28.0	9.50	--	--	390	1.1	43.0	--	3421	1942	--	119	5.0
154	39	4-28	29.0	9.08	--	223	363	2.1	29.6	--	6601	3747	49	129	--
158	40	4-29	29.0	9.25	--	166	268	2.8	23.3	--	5281	2998	81	126	3.0
162	41	4-30	29.5	9.25	--	145	162	2.3	15.2	11	3661	2078	--	117	1.9
169	42	5-1	29.5	9.1	--	186	118	2.0	12.3	--	3240	1839	--	--	--
172	42.5	5-1	30.0	9.77	--	187	106	4.2	13.8	--	3661	2078	86	--	--
174	43	5-2	29.5	10.04	--	235	113	3.5	17.4	11	4321	2453	--	--	--
175	--	--	--	--	--	197	--	0.4	16.0	--	1800	1022	--	--	--
177	43.5	5-2	29.5	9.20	--	273	112	3.6	18.3	--	4801	2725	--	121	0.3
179	--	--	--	--	--	276	88	2.2	11.1	--	--	--	--	--	--
180	44	5-3	29.0	9.4	--	267	103	2.0	18.9	10	5281	2998	100	126	--
183	44.5	5-3	--	--	--	265	98	2.0	18.5	--	5161	2929	--	--	--
186	45	5-4	29.0	9.5	--	257	82	2.0	17.8	--	5101	2895	--	--	--
189	45.5	5-4	29.5	9.5	--	262	80	2.1	17.8	--	4921	2793	107	121	0.3
192	46	5-5	29.0	9.4	--	257	72	2.0	16.0	--	4261	2418	--	--	--
196	47	5-6	29.0	9.2	--	270	81	1.5	15.8	--	5161	2929	--	--	0.4
200	48	5-7	29.0	9.4	--	262	72	0.8	15.9	--	4981	2827	--	122	--
208	49	5-8	29.5	9.4	--	253	92	2.3	13.8	10	5221	2963	114	--	--
211	49.5	5-8	29.5	9.5	--	256	93	2.4	13.7	--	5281	2998	--	--	--
215	50	5-9	29.5	9.5	--	238	103	2.5	13.7	--	5401	3066	--	--	1.2
218	50.5	5-9	28.5	9.4	--	238	110	2.5	1413	--	5401	3066	114	127	--
226	51	5-10	28.5	9.4	--	238	105	2.3	13.2	--	5221	2963	--	--	--
227	52	5-11	28.0	9.4	--	265	109	2.4	13.4	--	5281	2998	--	--	--
230	53	5-12	28.5	9.4	--	257	116	2.6	13.4	--	5461	3100	--	--	--
233	53.5	5-13	28.5	9.4	--	255	125	2.6	14.9	--	5461	3100	114	--	--
236	54	5-13	28.5	9.4	--	258	132	2.6	15.5	8	5701	3236	--	125	1.0
301	--	--	--	--	--	255	156	2.1	15.1	--	5941	3372	--	--	--
304	--	--	--	--	--	212	140	1.6	16.9	--	5161	2929	--	--	--
307	--	--	--	--	--	213	134	2.5	11.3	--	4621	2623	129	--	--
310	--	--	--	--	--	248	137	3.8	11.8	--	4621	2623	--	121	--
313	--	--	--	--	--	257	135	2.8	12.1	--	4681	2657	121	--	--

Table 8. Summary of Chemical Analyses for USBH-4

	Day	Date	T°C	pH	HCO_3^-	Na	K	Ca	Mg	SiO_2	CO_3^{2-}	NH_4	SO_4^{2-}	Cl	U
8	1	3-20	--	6.97	326	166	10.8	73	12	32	--	<0.1	--	177	0.1
13	2	3-21	26.5	7.18	308	165	10.9	72.5	12	--	--	<0.1	100	--	--
18	3	3-22	24.3	6.90	377	128	12.4	57	6	--	--	<0.1	--	--	--
22	4	3-23	26.0	7.40	341	136	10.7	51	7	--	--	<0.1	--	--	--
29	6	3-25	28	8.40	--	140	25.0	26	6	--	480	272	--	--	--
33	6.5	3-25	--	9.80	--	181	56.0	36	14	34	3720	2111	--	--	5
37	9	3-28	--	8.40	--	--	378	2.6	25	19	10741	6097	--	146	60
42	10	3-29	--	8.90	--	252	260	2.5	19	21	9241	5245	93	144	106
44	11	3-30	28.8	9.30	--	255	273	4.3	28	18	17522	9946	--	--	150.5
45	12	4-31	26.0	9.38	--	221	203	2.0	26	--	13022	7391	--	154	143
55	13	4-1	28.5	9.50	--	205	177	1.8	20	14	19803	11240	--	--	--
59	14	4-2	--	--	--	200	174	1.8	29	--	18602	10559	--	--	--
63	15	4-3	30.0	9.30	--	177	130	6.5	30	7	15722	8924	--	180	127.5
67	16	4-4	30.0	9.30	--	181	127	4.3	27	--	13682	7766	100	158	150.1
71	17	4-5	30.0	9.35	--	177	105	7.5	30	--	10501	5960	--	145	170.6
74	18	4-6	28.0	10.05	--	168	89	2.5	19	7	9481	5381	133	140	160.3
79	19	4-7	28.0	9.78	--	195	56	2.3	12.2	--	8581	4870	--	131	167.8
83	20	4-8	27.0	9.97	--	219	89	2.3	17.1	--	10141	5756	--	--	139.5
86	21	4-9	28.0	9.82	--	193	37	2.3	8.3	6	9961	5654	--	143	--
91	22	4-10	27.0	9.68	--	180	36	3.7	7.4	--	10381	5892	129	144	--
97	24	4-11	27.0	9.64	--	180	33	2.2	7.2	--	10621	6029	--	138	5
106	26	4-13	31.0	9.59	--	194	44	3.5	8.6	10	10261	5824	--	--	--
114	28	4-15	31.0	9.47	--	177	35	3.4	6.5	11	10021	5688	--	--	--
122	31	4-18	31.0	9.41	--	179	29	3.3	5.4	12	9901	5620	46	148	--
127	34	4-21	29.0	8.83	--	131	19	6.7	5.7	34	600	340	--	100	--
131	36	4-23	28.5	9.2	--	143	22	5.1	12.9	38	1080	613	--	106	5
137	37	4-24	28.5	8.58	--	130	18	31.2	12.5	--	683	357	--	--	--
140	38	4-25	--	9.33	--	130	19	8.1	9.3	36	660	374	73	100	1.6
145	39	4-26	28.3	8.48	--	142	19	26.9	13.2	38	480	272	--	--	--
150	40	4-27	28.5	8.32	--	118	19	26.0	9.6	--	482	275	--	181	--
156	41	4-28	29	7.49	342	119	18	63.0	10.0	32	--	278	--	--	--
160	42	4-29	28	7.25	342	119	16	30.2	10.0	40	--	273	61	--	--
164	43	4-30	28	7.69	320	125	18	30.7	10.3	36	--	274	--	99	--
197	49	5-6	28	7.20	320	141	18	30.0	11.6	36	--	272	--	103	--

Table 9. Summary of Chemical Analyses USBH-7

	Day	Date	T°C	pH	HCO_3^-	Na	K	Ca	Mg	SiO_2	CO_3^{2-}	NH_4	SO_4^{2-}	Cl^-	U
6	1	3-20	--	10.7	--	132	13.3	46.5	0.1	28	--	<0.1	114	84	0.09
12	2	3-21	--	11.2	--	134	13.5	19	0.3	--	--	<0.1	--	101	--
23	4	3-23	26.0	7.18	312	130	13.3	28	3.7	37	--	<0.1	--	72	--
34	6	3-25	--	7.30	363	127	12.3	34	5.1	--	--	<0.1	71	69	--
36	9	3-28	28.0	7.10	327	--	10.7	67.5	9.3	40	--	<0.1	--	73	--
43	10	3-29	27.8	7.15	341	122	11.5	57	--	--	--	<0.1	86	--	--
46	12	3-31	26.5	7.20	334	122	11.5	58	6.3	--	--	<0.1	--	73	--
54	13	4-1	26.0	7.40	341	120	11.2	60	6.5	--	--	<0.1	--	--	--
58	14	4-2	27.5	7.41	337	122	11.3	60.5	6.5	--	--	<0.1	69	--	--
60	15	4-3	26.0	7.39	341	122	11.2	61	6.7	--	--	<0.1	--	73	--
64	16	4-4	26.0	7.16	--	129	11.3	62	6.8	--	--	<0.1	--	--	--
68	17	4-5	24.0	7.50	--	123	10.8	63	6.9	--	--	<0.1	64	70	--
73	18	4-6	24.0	7.30	327	123	11.0	61.5	6.9	--	--	<0.1	--	--	--
76	19	4-7	24.0	6.95	334	117	9	48.4	7.2	--	--	<0.1	71	--	--
80	20	4-8	24.0	6.98	337	117	9	51.0	7.0	--	--	<0.1	--	71	--
84	21	4-9	24.0	7.10	339	115	10	48.5	7.0	--	--	<0.1	67	--	--
87	21.5	4-9	24.0	6.85	348	122	10	49.6	7.5	41	--	<0.1	--	--	--
88	22	4-10	24.0	6.70	392	130	11	51.0	8.1	41	--	<0.1	71	--	--
92	22.5	4-10	24.0	6.85	397	117	9	51.2	8.3	--	--	<0.1	--	81	--
93	23	4-11	24.0	6.50	494	118	9	61.0	10.7	--	--	<0.1	--	--	--
98	23.5	4-11	24.0	6.50	506	119	10	55.5	10.6	37	--	<0.1	71	--	--
100	24	4-12	24.0	6.12	634	125	10	54.0	13.8	--	--	<0.1	--	100	--
103	24.5	4-12	28.0	6.20	628	130	10	52.0	14.1	--	--	<0.1	64	--	--
104	25	4-13	28.0	6.10	762	180	13	52.0	17.5	39	--	<0.1	103	--	--
107	25.5	4-13	28.0	6.12	787	186	15	52.0	18.3	--	--	<0.1	86	--	--
108	26	4-14	28.0	6.16	848	197	15	61.0	18.4	--	--	<0.1	--	--	--
111	26.5	4-14	28.0	6.42	1147	246	18	55.5	20.5	--	--	<0.1	--	119	3.7
112	27	4-15	28.0	7.20	1366	270	23	45.0	21.1	38	--	0.1	--	--	--
115	27.5	4-15	28.0	8.62	--	334	40	24.2	26.1	38	1680	954	100	--	--
116	28	4-16	28.0	8.91	--	276	79	1.2	27.0	44	2160	1226	--	108	--
118	29	4-17	28.0	9.14	--	265	92	1.6	26.8	32	2100	1192	--	--	--
121	30	4-18	28.0	9.26	--	186	112	0.5	25.2	--	2220	1260	--	--	13.6
123	31	4-19	28.0	9.31	--	194	114	0.4	24.0	32	720	409	89	111	15.5
126	33	4-21	28.0	7.58	695	--	30	6.7	9.2	33	--	273	--	104	1.0
130	35	4-23	28.0	7.80	--	131	18	28.0	7.8	--	--	270	57	--	0.5
138	36	4-24	28.0	7.60	329	129	13	43.8	8.8	--	--	280	--	--	0.3
139	37	4-25	28.0	7.68	376	123	19	11.2	8.0	--	--	250	77	--	0.2
146	38	4-26	28.0	9.25	--	164	71	1.2	15.2	28	1560	886	--	--	--
147	39	4-27	28.0	9.40	--	178	92	1.2	18.1	--	1860	1056	--	--	5
153	40	4-28	29.0	9.15	--	164	82	0.2	19.0	30	1440	817	100	109	--
159	41	4-29	29.0	9.09	--	153	68	2.0	17.0	--	1380	783	--	108	3
163	42	4-30	29.0	9.30	--	196	60	0.3	19.8	23	1740	988	93	--	--
166	42.5	4-30	29.0	9.10	--	191	70	0.3	18.3	--	1500	852	--	--	2.3
167	43	5-1	29.0	9.35	--	200	62	0.3	17.0	--	1800	1022	--	--	--
170	43.5	5-1	29.0	9.70	--	186	69	0.8	15.4	20	1800	1022	--	--	--
175	44	5-2	29.5	9.70	--	200	64	0.7	15.9	--	1920	1090	91	--	2
176	44.5	5-2	29.0	9.32	--	200	68	2.0	14.8	--	1680	954	--	110	--
181	45	5-3	29.0	9.50	--	186	59	2.0	14.2	--	1980	1124	--	--	--
182	45.5	5-3	29.0	--	--	191	63	0.3	13.4	--	1440	817	--	--	1.4
187	46	5-4	29.0	--	--	184	53	5.4	15.4	--	2280	1294	79	--	--
188	46.5	5-4	29.0	9.40	--	212	76	0.4	15.5	19	1560-	886	--	--	--
193	47	5-5	28.5	9.30	--	193	58	0.8	16.5	--	1260	715	--	--	--
198	48	5-6	29.0	9.30	--	150	42	0.7	15.2	--	2160	1226	83	106	0.5
199	--	--	--	--	--	220	67	2.6	15.4	--	1740	988	--	--	--
212	50	5-8	29.0	9.40	--	240	--	0.1	15.4	28	1980	1124	--	--	--
214	51	5-9	29.0	9.50	--	219	11	0.9	17.1	--	2220	1260	--	110	0.6
219	51.5	5-9	28.0	9.40	--	232	77	0.3	17.5	--	1560	886	93	--	--
220	52	5-10	28.5	9.30	--	201	59	0.4	16.0	23	1920	1090	--	--	--
225	52.5	5-10	28.0	9.30	--	230	73	0.4	16.3	--	1680	954	--	--	--
226	53	5-11	28.0	9.40	--	220	62	0.4	16.3	--	--	--	--	--	0.4
231	53.5	5-12	28.0	9.30	--	292	75	0.2	21.3	--	2160	1226	77	--	--
232	54	5-12	28.0	9.30	--	219	80	0.1	20.4	--	2220	1260	--	--	--
237	55	5-13	28.0	9.40	--	230	85	0.6	28.5	21	2400	1363	--	111	0.5
275	--	--	--	--	--	213	71	0.2	16.0	--	2040	1158	93	--	--
300	--	--	--	--	--	238	80	0.4	29.3	--	2160	1226	--	--	--
305	--	--	--	--	--	158	48	0.4	24.0	--	1740	988	--	--	--
306	--	--	--	--	--	159	47	0.6	29.2	--	2160	1226	--	--	0.5
311	--	--	--	--	--	197	72	0.3	24.0	--	1200	681	51	--	--
312	--	--	--	--	--	193	77	0.7	23.9	--	3060	1737	66	114	0.5

Initially the water arriving at the wells was displaced formation water. If the flow is slug flow as assumed by various hydrologic models used for modelling (Shock, 1977) then one would expect to see an increase in pH, NH_4 concentration and CO_3^- concentration as the lixiviant arrives at the well. Slug flow would result in all of the ions arriving more or less at the same time. If the diffusion rate of an ionic species is greater than the flow rate, the ionic species could arrive early. However, because of the relatively slow diffusions rates of most ions, this is unlikely. In addition, if an ionic species is specifically adsorbed on the surface of the mineral grains, it will be retarded in its arrival with respect to an ionic species which does not adsorb on surfaces. Specific adsorption would allow for a chromatographic separation of ions in the moving lixiviant and invalidate assumptions regarding slug flow. The phenomenon of ions being separated or arriving at different times was indeed observed, particularly in USBM-7 which had the longest arrival time for the fluid. Figures 7, 8, 9, 10, and 11 illustrate the various arrival times of the moving lixiviant as indicated by changes in various chemical parameters. Based on these data, it would appear that migration rates decrease in the order $H > HCO_3 > Mg > Cl > Na > K > Ca > NH_4$, or that the relative adsorption of the ions increases in the same order.

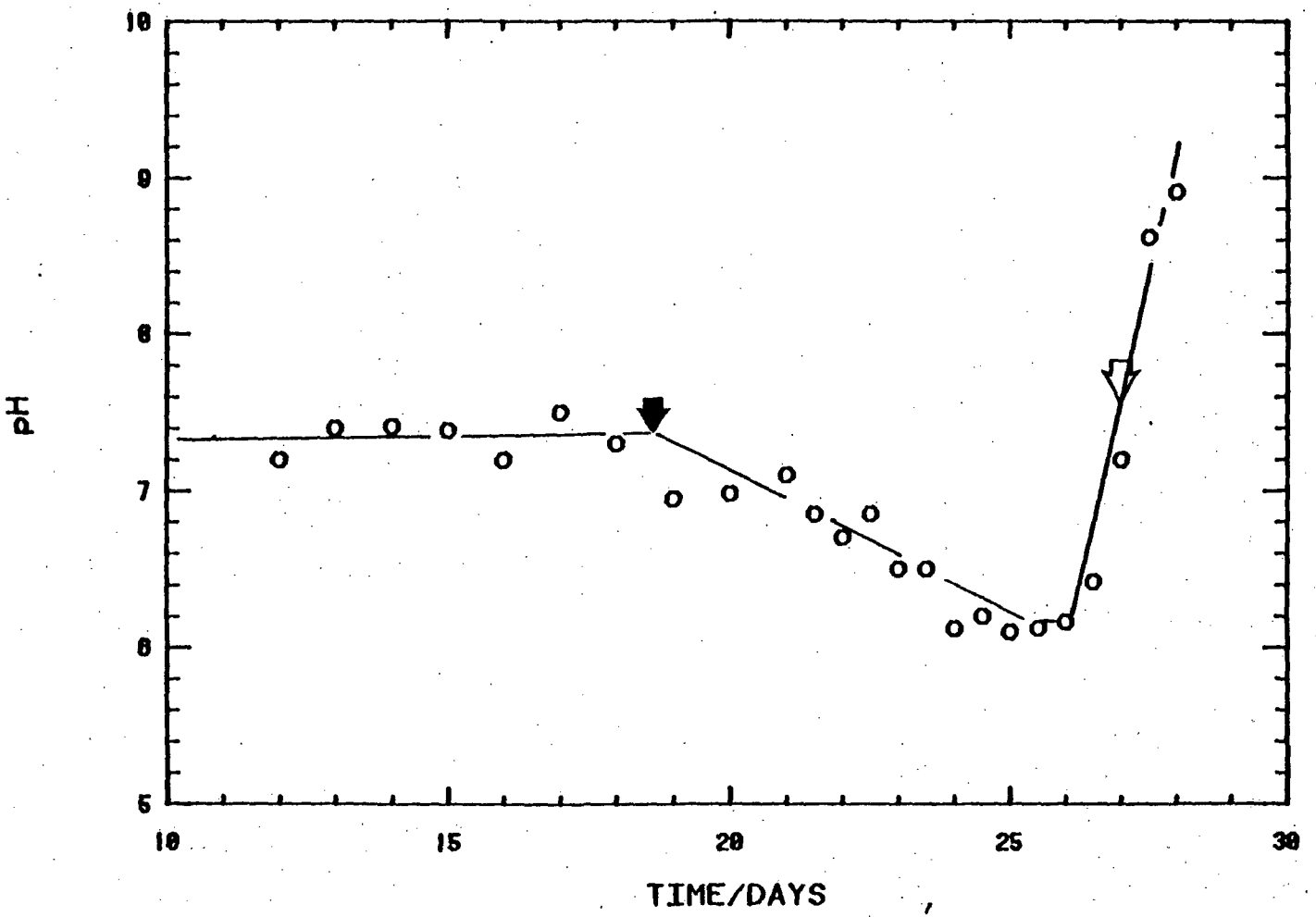

Figure 7. pH as a function of time. Solid arrow indicates the arrival of H^+ while the open arrow indicates the arrival of the first detectable NH_4^+.

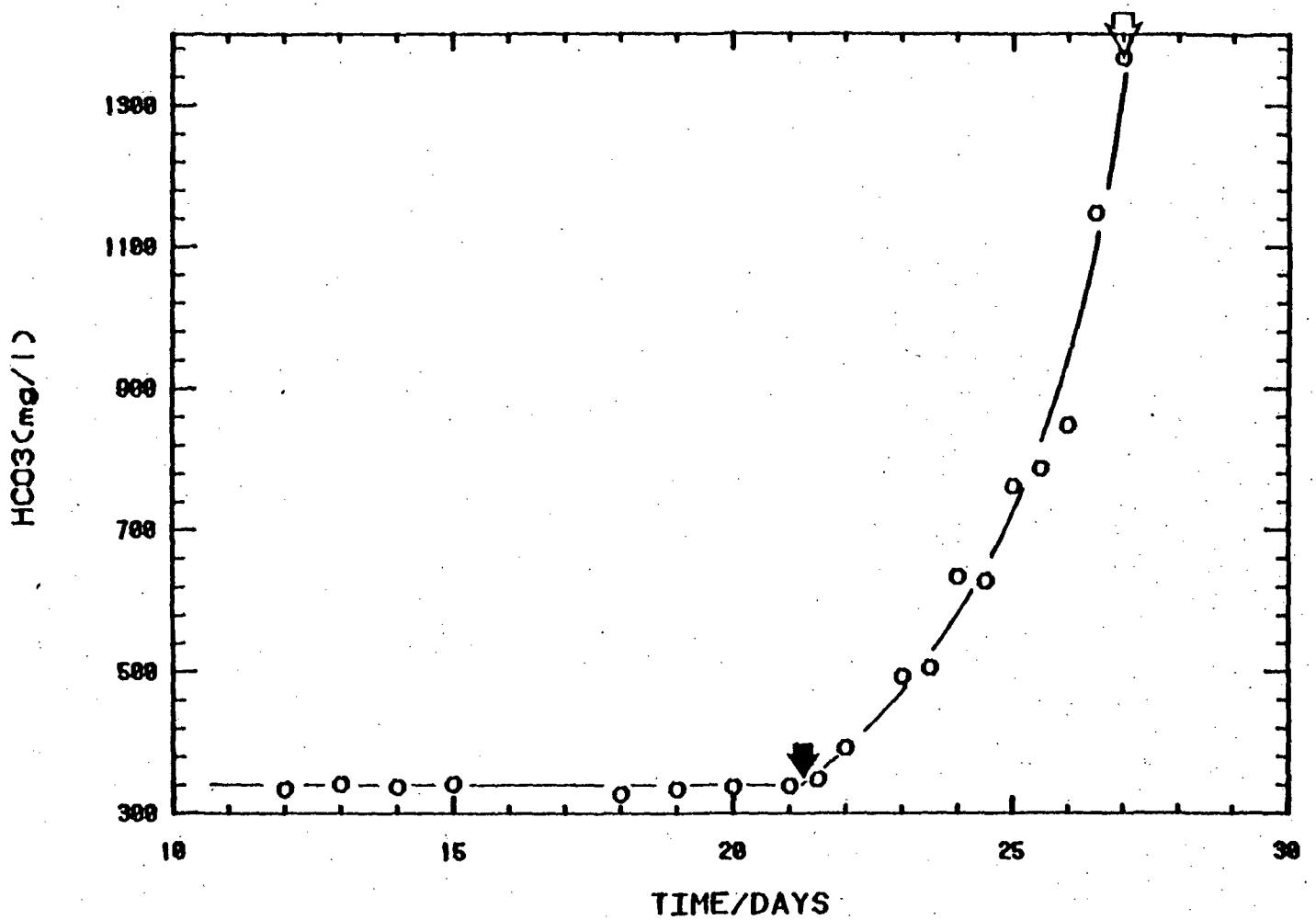

Figure 8. HCO_3^- concentration as a function of time. Solid arrow indicates the arrival of HCO_3^- while the open arrow indicates the arrival of the first detectable NH_4^+.

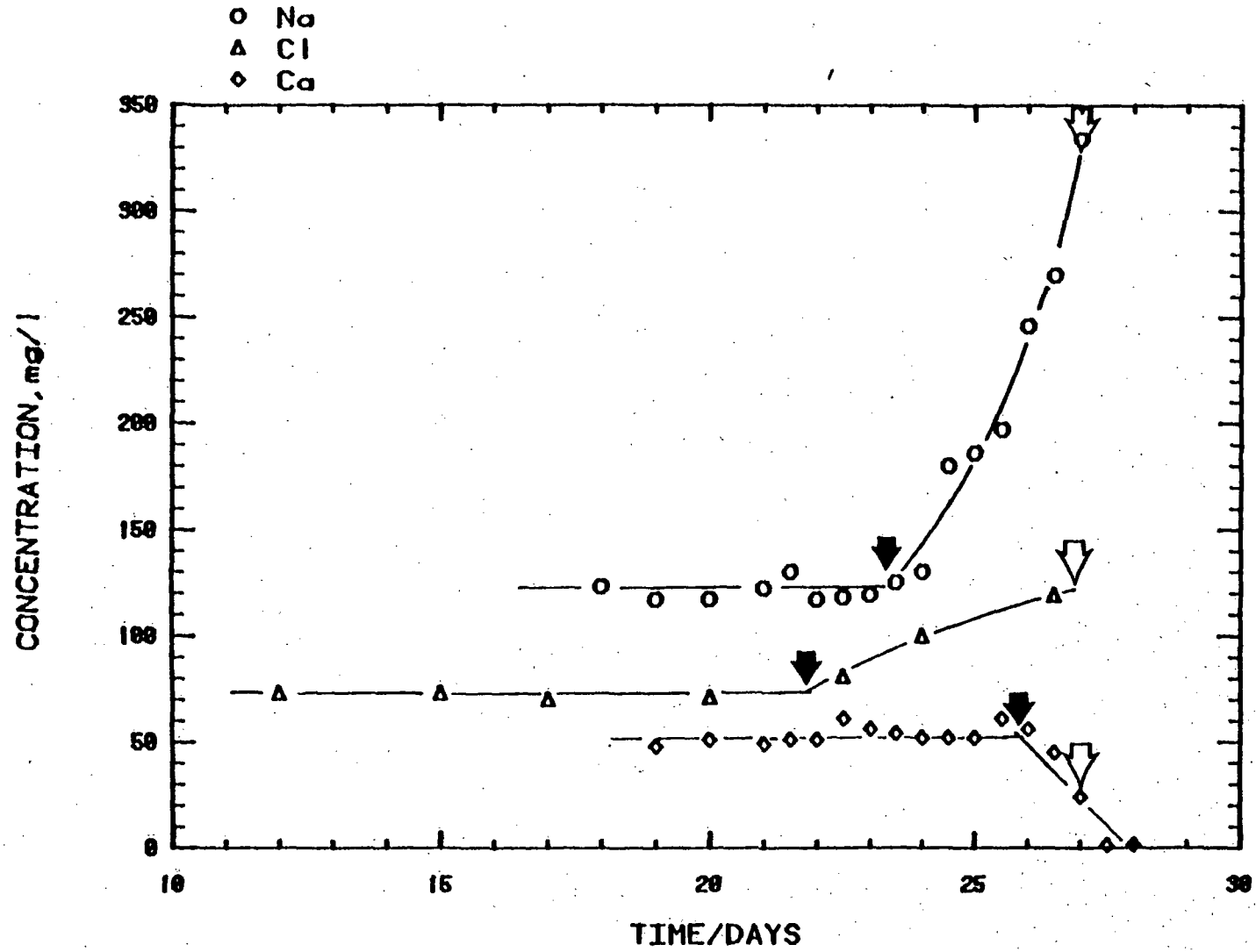

Figure 9. Na^+, Cl^-, and Ca^{++} concentration as a function of time. Solid arrows indicate the arrivals of Na^+, Cl^- and Ca^{++} while the open arrow indicates the arrival of the first detectable NH_4^+.

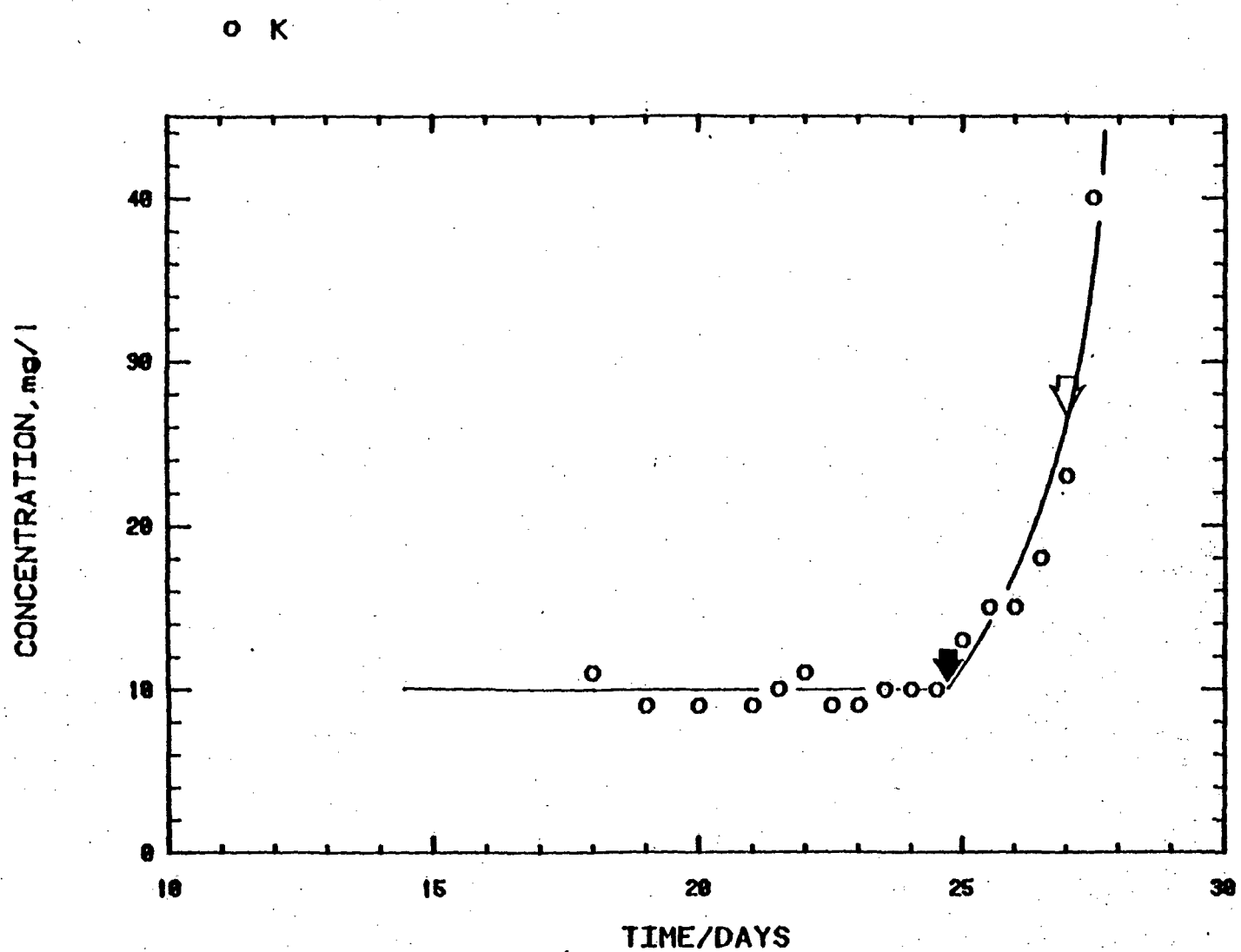

Figure 10. K^+ concentration as a function of time. Solid arrow indicates the arrival of K^+ while the open arrow indicates the first arrival of detectable NH_4^+.

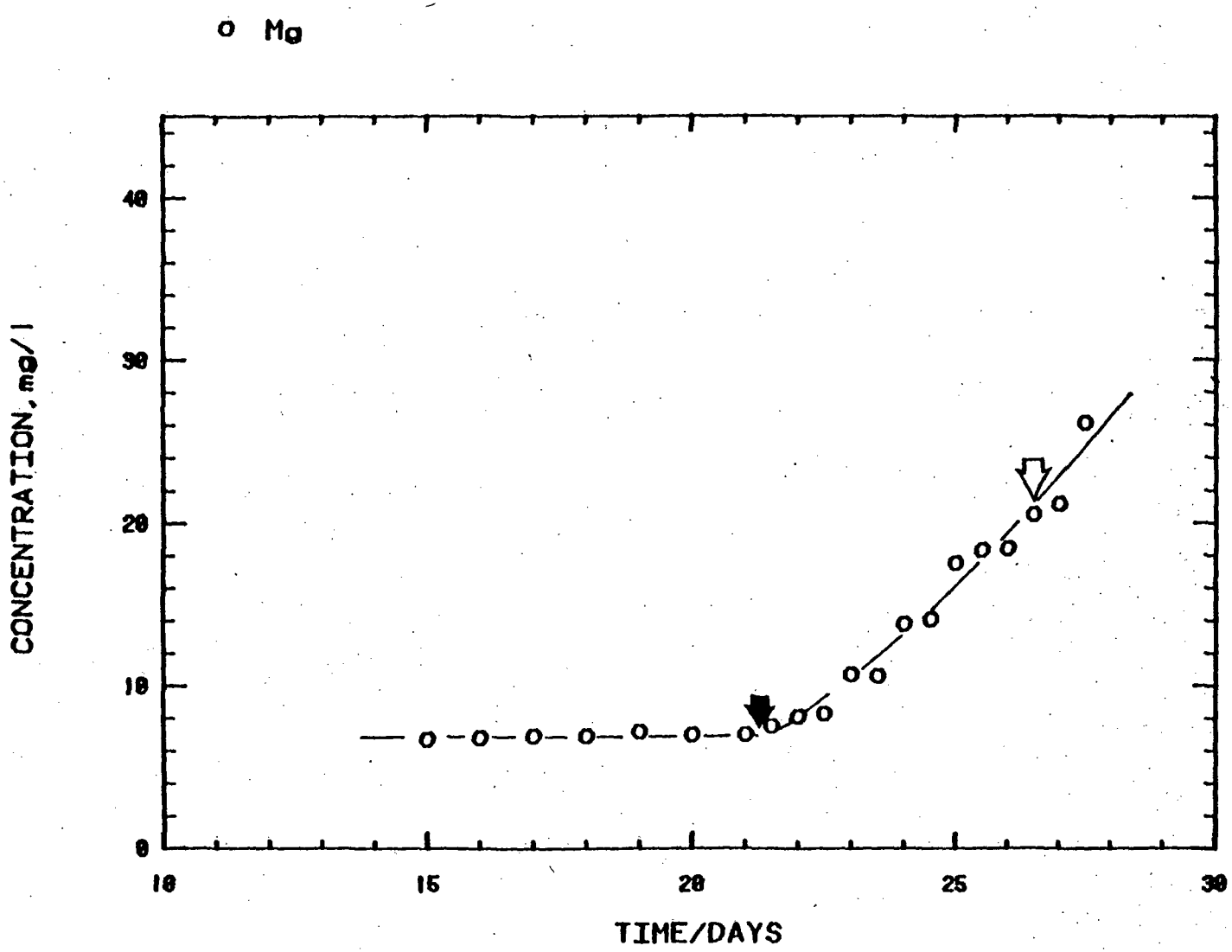

Figure 11. Mg^{++} concentration as a function of time. The solid arrow indicates the arrival of Mg^{++} while the open arrow indicates the first arrival of detectable NH_4^+.

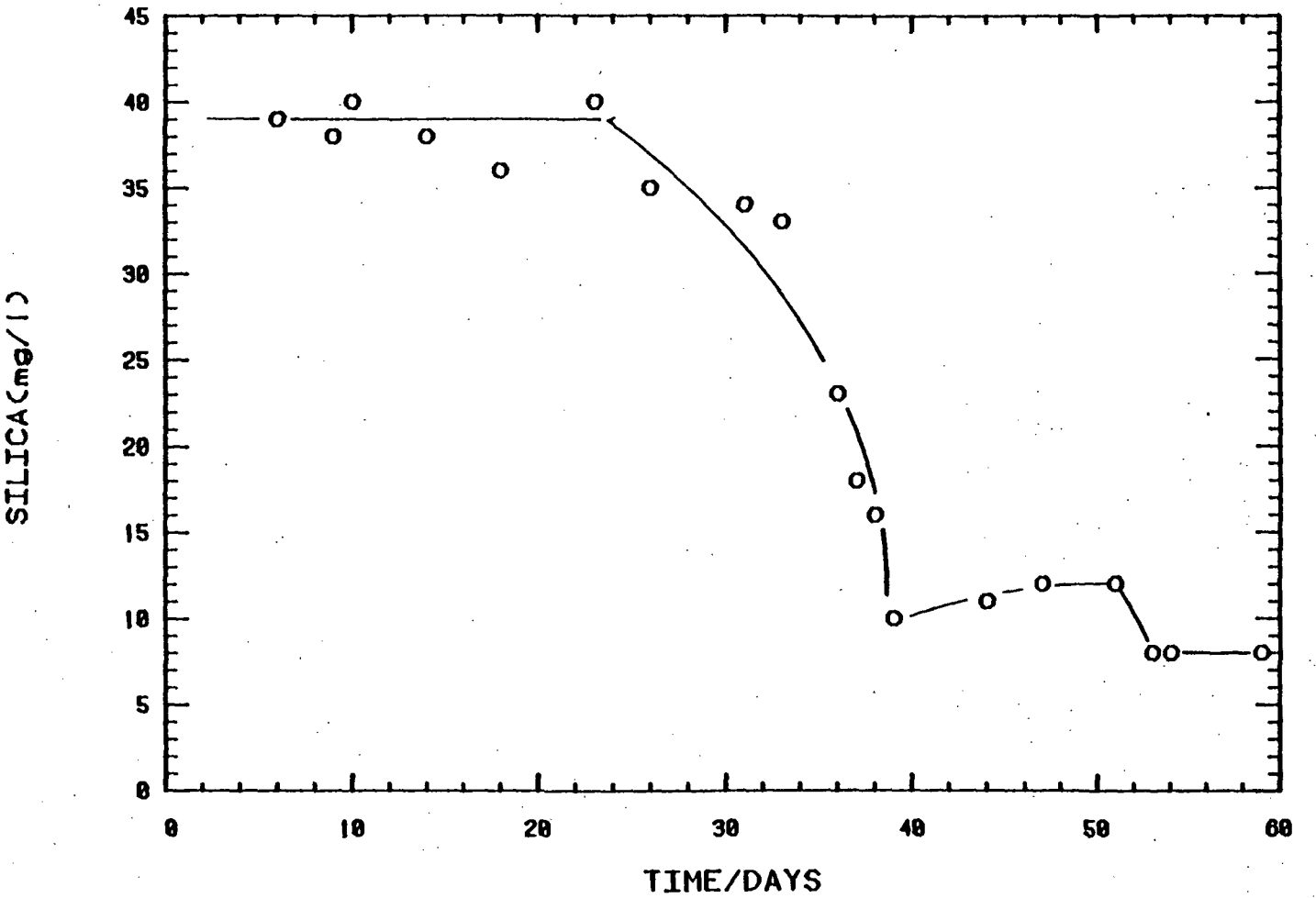

Figure 12. The SiO_2 concentration as a function of time for USBM-1, illustrating the unexpected decrease in silica concentration.

Several other interesting phenomena occurred with respect to changes in the concentration of various elements during the leaching phase. The lixiviant with only air as an oxidant successfully mobilized uranium near the injection points which were in the oxidized zone. However, as these solutions moved outward, the uranium content decreased significantly. This phenomenon would be expected in the reduced region of the ore deposit, but was unexpected in the oxidized portion. There are several possible explanations for the behavior of uranium in USBM-7:

1. Uranium migration is slower than that of the other elements (except NH_4). The direction of the flow in the field was reversed on 4/19 and the maximum uranium concentration may not have been achieved.

2. Slower migration of uranium indicates its selective adsorption on clays and zeolites. Significant adsorption and/or ion exchange may have occurred, thus reducing the uranium concentration.

Using SOLMNEQ and WATEQ, saturation with various silicate phases was again calculated using an average groundwater composition plus the appropriate concentration of ammonium carbonate. On the basis of these calculations one would predict that the concentration of silica would remain unchanged or increase slightly since the stability of most of the silicate phases had decreased. As can be seen in figure 12, the response was just the opposite of what was expected: the silica concentration showed a marked decrease. Only in one well,

USBM-4, did the silica ever regain its former concentration; this was however, associated with the reversal in the flow direction and the subsequent hydrologic isolation of USBM-4. The decrease can seemingly only be related to the formation of a silicate phase not contained in the computer codes such as buddingtonite (NH_4 feldspar) or some similarly related form. The reaction of the ammonium carbonate plus silica with the clays could yield the ammonium feldspars plus hydrogen ion which could explain the source of the early arriving hydrogen ion detected in the various wells.

The Na, K, and Mg concentrations are more strongly controlled by ion exchange reactions than by chemical equilibria involving dissolution and precipitation except possibly for some contribution from the reaction of montmorillonites with the lixiviant to form ammonium feldspars. The concentration of all three elements increases in the lixiviant in such a way as to suggest a preferential release of Mg >K > Na, although due to the observed chromatographic effects this preferential or kinetic exchange reaction can not be confirmed without laboratory experiments designed to separate kinetic from chromatographic effects.

The behavior of Ca at first glance is somewhat predictable; i. e., as the CO_3 content increases the Ca concentration decreases. However the decrease in Ca is not as rapid as would be expected and the resulting concentrations appear to be in approximate equilibrium, slightly supersaturated or in a few cases extremely supersaturated

with respect to calcite. These observations appear to indicate that either the kinetics of $CaCO_3$ precipitation are responsible for the slow decline or Ca is being added by ion exchange at or near the same rate as the precipitation of $CaCO_3$. The behavior of Cl during the leaching operation is an almost perfect example of homogenization of a chemical gradient. The make up water had a slightly higher Cl concentration than USBM-1, USBM-3, and USBM-7 and a lower concentration than USBM-4. With time all four wells approached a uniform value, except for USBM-7 which showed fluctuations due to the reversal of flow in the field.

The SO_4 concentration shows a progressive increase with time in all wells. The largest increase was noted in USBM-1 after the reversal of flow in the field and after H_2O_2 had been injected into the formation. These increases are due to the oxidation of pyrite by the oxidant. A concomitant increase in Fe concentration was not detected; however, at these high pH values one would expect the Fe to precipitate as amorphous iron oxi-hydroxide, and thus not be detected at the observation wells.

During the course of the leach operation there were no statistically significant variations of the concentrations of Al, Li, F, or B. This may be partially due to analytical problems for Al, Li, and F which were near their detection limits. The B concentration most likely indicates that it behaves as a conservative element throughout the leaching processes.

Although prior to the arrival of the lixiviant, the Eh electrode produced reasonably stable values; after the arrival of the lixiviant the readings became erratic. This behavior may have been related to the large increase in ionic strength of the fluids or because of fouling of the platinum electrode by the ammonia solution and/or fine suspended precipitates (gels) such as iron oxi-hydroxides, clays, etc. In conjunction with the problems related to the Eh electrode, an extremely high failure rate was observed for pH electrodes after the lixiviant began arriving. The cause for the electrode failures appeared to be clogging of the frit with fine grained particulates, which might also relate to the failures of the Eh combination electrodes as well.

During the course of the leaching of the orebody, the temperature of the lixiviant being produced from the sampling well systematically increased with time. The temperatures were initially about 25°C and slowly drifted up to around 31°C. This phenomena is of a greater magnitude than would be expected from chemical dissolution and precipitation reactions. The dissolution of $(NH_4)_2CO_3$ in water is endothermic which produces an opposite temperature change than was noted.

Comparison of Field Versus Laboratory Analyses:

The field determination of pH and HCO_3 are the most accurate methods for determining these quantities, since they are interdependent and cannot be preserved. Proper preservation methods exist for Na, K, and Ca; hence, if any field analytical method for these constituents is to be of any practical use, it must be capable of accurately reproducing the real values for the concentration. Figures 13, 14, and 15 illustrate the field data plotted versus the laboratory values for Na, Ca, and K respectively, for samples where the lixiviant had yet to arrive. The analyses done by field titration with EDTA for Ca appear to be the best with 56% of the measured values within ±10% of the atomic adsorption spectroscopy (AAS) values and with 74% of the measured values within ±20% of the AAS values. The next most reliable set of field analyses were the Na+ analyses done by ion-selective electrode. For Na, 51% of the analyses lie within ±10% of the AAS values while 84% of the values lie within ±20% of the AAS values. The worst field method appears to be the K analyses done by ion-selective electrode. Only 39% of the field measured values lie within ±10% of the AAS values and only 59% lie within ±20% of the AAS values.

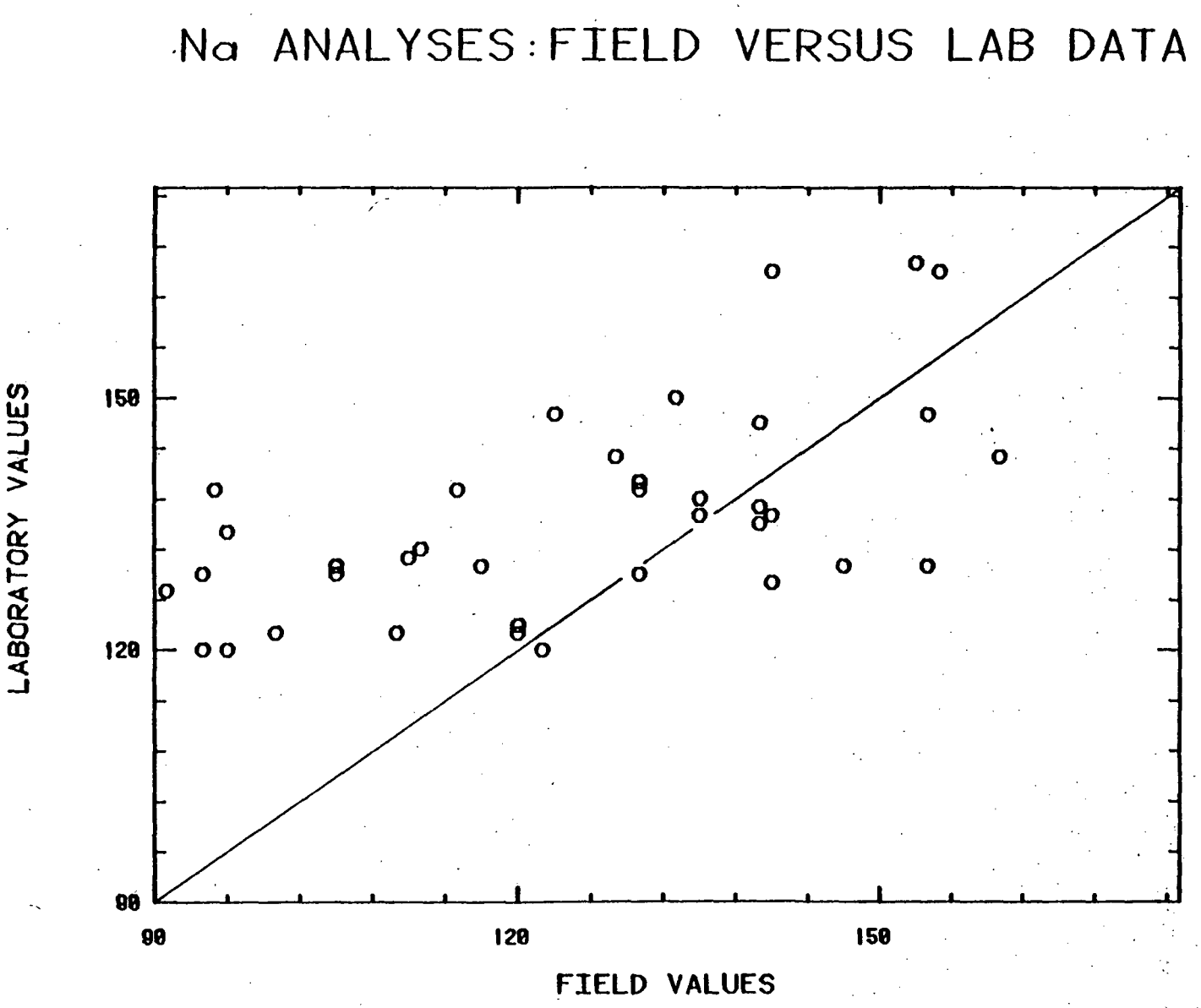

Figure 13. Comparison of field analytic data with laboratory data before arrival of lixiviant.

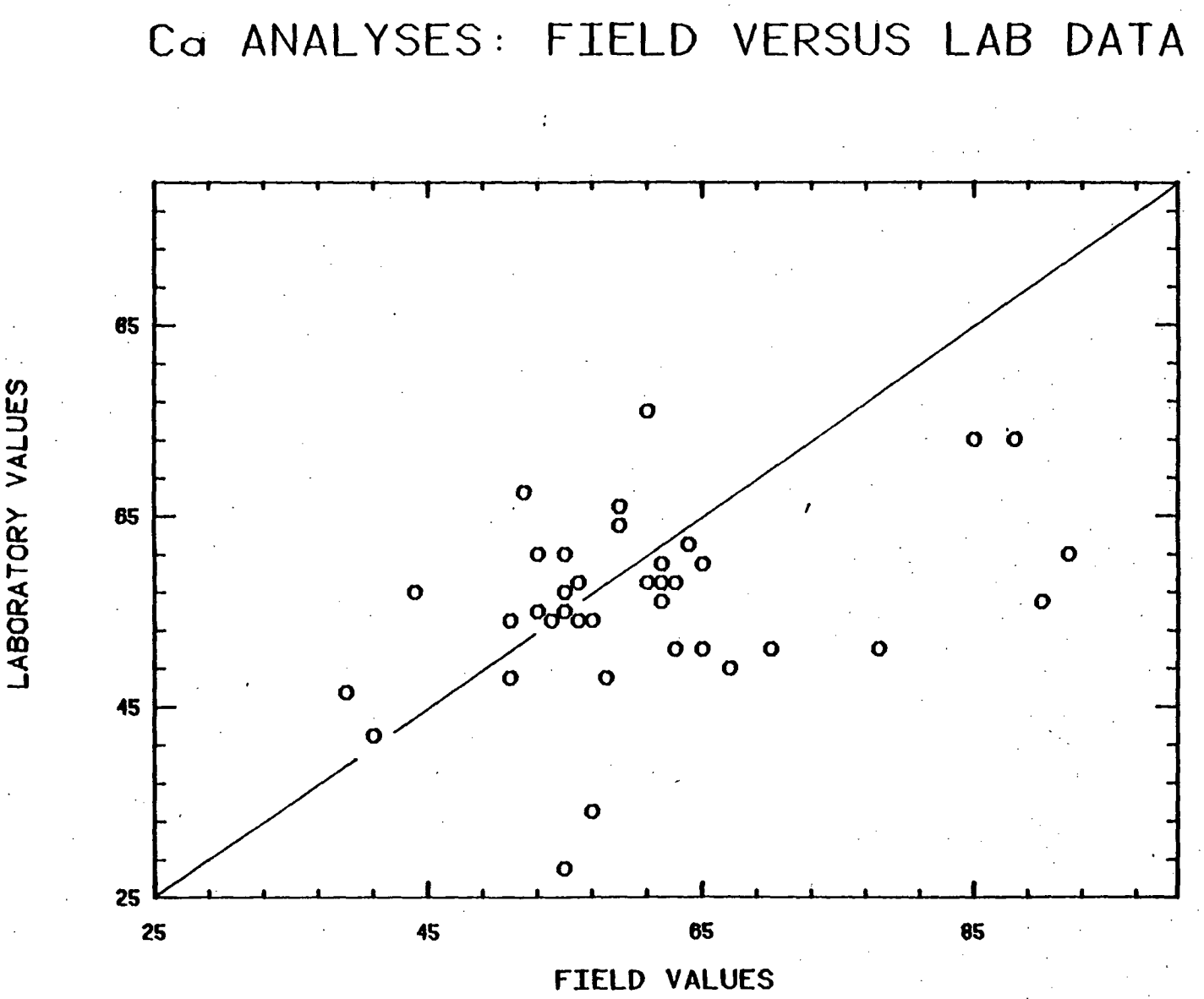

Figure 14. Comparison of field analytic data with laboratory data before arrival of lixiviant.

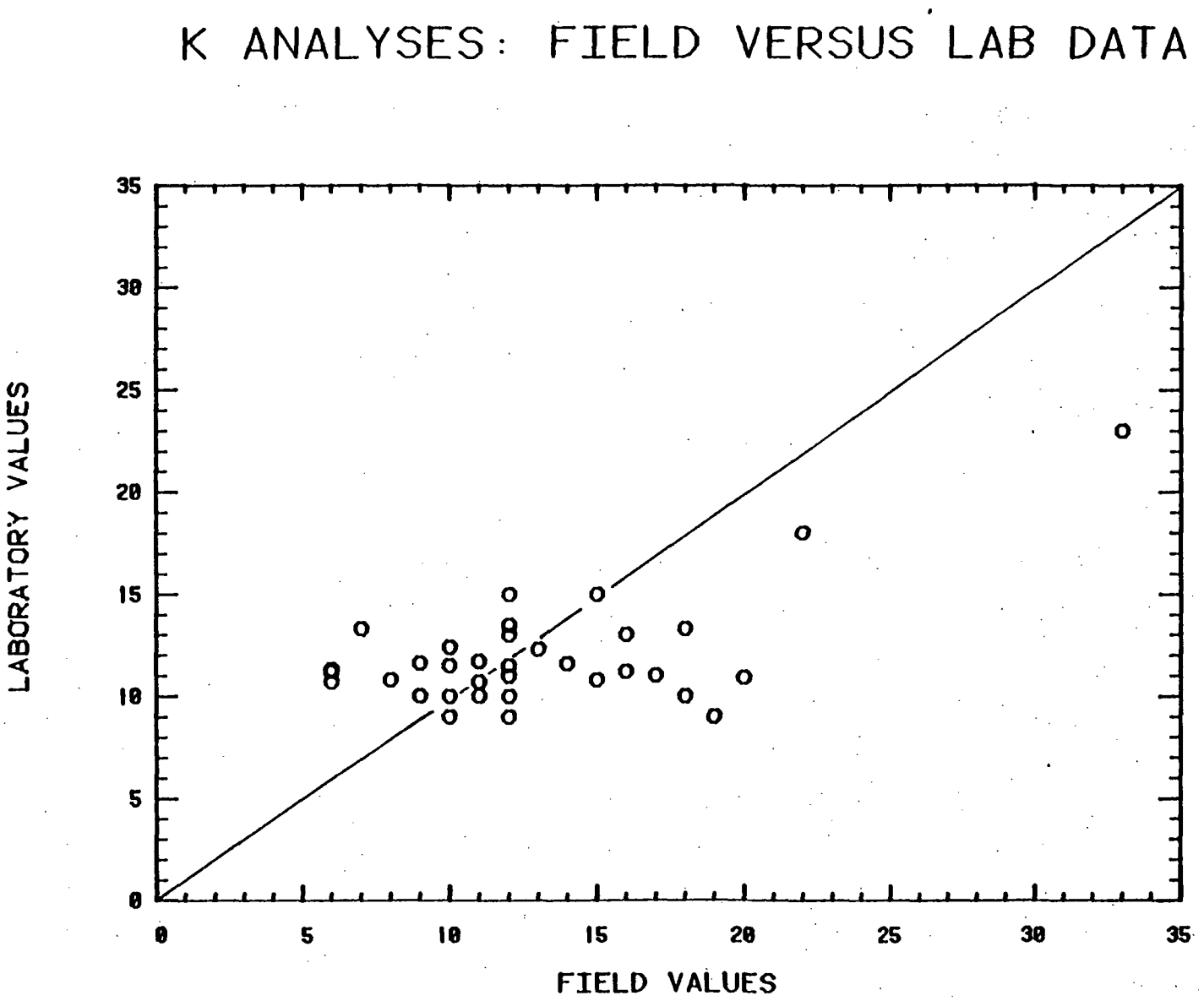

Figure 15.. Comparison of field analytic data for K^+ and laboratory data before arrival of lixiviant.

After the arrival of the NH_4 the reliability of the field analytical data dramatically decreased except for the K analyses which actually improved. The Ca analyses, which had been the best, suddenly became the worst with discrepancies commonly of an order of magnitude. This probably relates to the increasing concentration of Mg as well as the dissolution of fine grained (<0.1 micron) $CaCO_3$ by the EDTA as the values measured in the field are uniformly too high. The reliability of the Na electrode decreased markedly with only 45% of the measured values being within ±20% of the AAS values. The K electrode, however, improved its reliability slightly with 65% of the field measured values being within ±20% of AAS values. There appears to be no rational explanation for this behavior of the K electrode except that perhaps the field measured values are fortuitously closer to the real concentration.

In general, the results of the field analytical data for Na, K, and Ca are not encouraging. The data at best are only qualitative, particularly after the lixiviant arrives. The behavior of the Na electrode can be improved by the addition of NH_4 to the standards but the results do not warrant the extra effort. In contrast, the field pH and HCO_3 measurements are very reliable and could be employed with monitor wells to detect an excursion many days prior to NH_4 reaching the monitor well; thus allowing for the early corrective action to be taken.

CONCLUSIONS

This report presents data on the chemical changes occurring during the in-situ leaching of an uranium orebody which has been well characterized mineralogically prior to leaching. These data hence constitute a data set against which any models for describing the leaching of an uranium orebody may be tested for reliability. These data also suggest areas which warrant further study:
(a) characterization of the chromatographic separation of ions, (b) kinetics of the ion-exchange of the clay minerals, (c) the influence of zeolites on exchange and chromatographic behavior of ions, (d) the ion-exchange capacity of zeolites and clays for uranium, (e) the kinetics and thermodynamics of the oxidation of uranium minerals by various oxidants, and (f) studies centered on the methodology for extracting the NH_4 which has been ion exchanged and/or reacted with the host formation. The later area of research would require as a companion to detailed laboratory work, a comprehensive study of the restoration to initial baseline conditions of a leached uranium orebody similar to the study summarized in this report. In light of the complexities encountered during the leaching of this orebody, similar studies of other types of orebodies should be conducted for both the alkaline and acid leaching systems.

REFERENCES

Barnes, Ivan, 1964, Field measurement of alkalinity and pH: U.S. Geological Survey Water-Supply Paper 1545-H, 17 p.

Kharaka, Y. K., and Barnes, Ivan, 1973, SOLMNEQ: Solution-mineral equilibrium computations: U.S. Geological Survey Computer Center, U.S. Department of Commerce, National Technical Information Service, Springfield, Virginia 22151, Report PB-215899, 82 p.

Shock, D. A., 1977, The Vail Conference on in-situ leaching of uranium In-Situ, v. 1, p. 103-113

Truesdell, A. H., and Jones, B. F., 1974, WATEQ, a computer program for calculating chemical equilibria of natural waters: U.S. Geological Survey Journal of Research, v. 2, p. 233-248.